NATIONAL ADVISORY COMMITTEE FOR AERONAUTICS

TECHNICAL NOTE

No. 1275

A LIFTING-SURFACE-THEORY SOLUTION AND TESTS OF AN ELLIPTIC

TAIL SURFACE OF ASPECT RATIO 3 WITH A

0.5-CHORD 0.85-SPAN ELEVATOR

By Robert S. Swanson, Stewart M. Crandall, and Sadie Miller

Langley Memorial Aeronautical Laboratory
Langley Field, Va.

Washington

May 1947

NATIONAL ADVISORY COMMITTEE FOR AERONAUTICS

TECHNICAL NOTE NO. 1275

A LIFTING-SURFACE-THEORY SOLUTION AND TESTS OF AN ELLIPTIC

TAIL SURFACE OF ASPECT RATIO 3 WITH A

0.5 CHORD 0.85-SPAN ELEVATOR

By Robert S. Swanson, Stewart M. Crandall, and Sadie Miller

SUMMARY

An electromagnetic-analogy model of the vortex load, esti-
mated from lifting-line theory with an arbitrary fairing near the
elevator tip, on a thin elliptic horizontal tail surface of aspect
ratio 3 with a 0.5-chord 0.85-span plain elevator was constructed
and tested. The aspect-ratio corrections to the lift and hinge
moments were calculated from the measured results.

A comparison of the aspect-ratio corrections for the partial-
span elevators was made with those previously presented for full-
span elevators. The comparison indicates that the incremental
difference in the lift parameters between the full-span and the
partial-span elevators may be estimated satisfactorily by lifting-
line theory. The incremental difference for the curve of hinge-
moment coefficient against angle of attack is usually small. Only
about 10 percent of the incremental difference for the slope of the
curve of hinge-moment coefficient against elevator deflection is
given by lifting-line theory; the total lifting-surface-theory
increment is -0.0009 per degree for the configuration considered.

Wind-tunnel results for a tail surface of the same plan form
are presented. The differences in estimated lifting-surface aspect-
ratio corrections for the full-span and the partial-span cases were
checked satisfactorily by the experimental data. A few tests with
a cut-out for the rudder were also presented. The effects of the
cut-out on the hinge-moment characteristics were large.

INTRODUCTION

A method was presented in reference 1 for estimating the finite-
span values of the lift and hinge-moment parameters of full-span

elevators from the section data. The present investigation was
undertaken in order to provide some data from which the lift and
hinge-moment parameters for partial-span elevators could be esti-
mated. The case presented is that of a thin elliptic horizontal
tail surface of aspect ratio 3 with a 0.5-chord 0.85-span plain
elevator.

References 1 and 2 showed that it is necessary to use lifting-
surface-theory aspect-ratio corrections to estimate satisfactorily
the finite-span hinge-moment parameters. Lifting-surface-theory
solutions are usually determined by a rapidly converging process
of successive approximations, of which the first approximation is
the lifting-line-theory solution. For partial-span elevators or
flaps, however, the contour lines of constant circulation strength
(see references 3 and 4) calculated by means of lifting-line theory
have abrupt discontinuities near the elevator tip, as shown by the

contour lines of the circulation function $\dfrac{\Gamma}{\Gamma_{max}}$ in figure 1. Since

such sharp bends in the contour lines are smoothed out by aerodynamic
induction, a more satisfactory loading may be obtained for the next
approximation by arbitrarily fairing the contour lines so that they
are smooth in the region just upstream of the elevator tip. The
contour lines on the elevator itself are smooth and therefore need
not be altered. In order to obtain some idea of the best means of
accomplishing this fairing, the three-dimensional pressure-distribution
data of reference 5 for a rectangular wing with partial-span split
flaps were integrated to obtain contour lines of constant circulation
strength. For comparison, the contour lines for the experimental
span loading, divided into flap-type and angle-of-attack-type
loadings (reference 6) by use of the principles of lifting-line
theory, were also constructed. Both sets of contour lines are given
in figure 2. In figure 3 are presented the contour lines of figure 1
refaired similarly to the contour lines of the experimental data
presented in figure 2.

An electromagnetic-analogy model having the contour lines of
figure 3 was then constructed and tested. The incremental lifting-
surface-theory aspect-ratio corrections were determined by calculating
the increments of chordwise and spanwise loading that would result
for a lifting surface shaped to correspond to the difference between
the measured downwash and the downwash determined from the two-
dimensional theories for the same contour pattern (fig. 3). In the
calculation of the increments of the lift and hinge-moment parameters
(additional aspect-ratio corrections), the difference between the
downwash measured for the faired contour pattern of figure 3 and the
downwash calculated from the 2 two-dimensional theories for the same
contour pattern are assumed to be nearly equal to the corresponding

difference in the measured and calculated downwash for the contour
pattern of figure 1.

In order to provide an experimental check of the aspect-ratio
corrections, some wind-tunnel tests were made of a model of the same
plan form and of NACA 0009 airfoil section, with both full-span and
partial-span elevators. The results, together with some additional
data showing the effect of elevator cut-outs, are presented in
appendix A.

The hinge-moment corrections for "feeler ailerons" (small-span
wide-chord ailerons at the wing tips) designed to provide the stick
feel for thin-plate, retractable-type, lateral-control devices are
of current interest. In order to provide some data for these arrange-
ments, the hinge-moment aspect-ratio corrections for a 0.5-chord
0.15-span feeler aileron on a wing of aspect ratio 3 are briefly
summarized in appendix B.

SYMBOLS

Γ circulation strength

C_L lift coefficient

c_l section lift coefficient

c_h section hinge-moment coefficient

C_h hinge-moment coefficient

a_o section slope of lift curve, per radian

α angle of attack

α_e effective angle of attack, radians $\left(\dfrac{c_l}{a_o}\right)$

α_o two-dimensional angle of attack

δ elevator deflection

δ_t tab deflection

w   vertical component of induced velocity

E   Jones edge-velocity correction factor for lift (reference 7)

E_{e_f} effective edge-velocity correction for lift of elliptic wing
          with partial-span flap (see references 1 and 7)

V   free-stream velocity

x   chordwise distance from wing leading edge

x_o chordwise distance from wing leading edge to point at which
          downwash is desired

y   spanwise distance from plane of symmetry

c   chord

c_s center-section chord

$\bar{c}_e$ root-mean-square chord of elevator

b   span of tail

ϕ trailing-edge angle, degrees

q   dynamic pressure

S   area of tail

b_e span of elevator

A   aspect ratio $\left(b^2/S\right)$

F   hinge-moment factor for theoretical load caused by streamline-
          curvature correction (reference 1)

η experimentally determined reduction factor for F to include
          the effects of viscosity (reference 1)

Δ increment

Δ' increment of parameter; value for elevator with full-span
          flap minus value for elevator with partial-span flap

Δ''   increment of parameter; value for elevator with no cut-out
minus value for elevator with cut-out

Parameters:

$c_{l_{\alpha}}$ $\left(\partial c_l / \partial \alpha_o\right)_{\delta} = a_o$

$c_{l_{\delta}}$ $\left(\partial c_l / \partial \delta\right)_{\alpha_o}$

$\left(\alpha_{\delta}\right)_{c_l}$ $\left| \left(\dfrac{\partial \alpha_o}{\partial \delta}\right)_{c_l} \right| = \dfrac{\left(\partial c_l' / \partial \delta\right)_{\alpha_o}}{\left(\partial c_l / \partial \alpha\right)_{\delta}}$

$\left(\alpha_{\delta}\right)_{C_L}$ $\left| \left(\dfrac{\partial \alpha}{\partial \delta}\right)_{C_L} \right| = \dfrac{\left(\partial C_L / \partial \delta\right)_{\alpha}}{\left(\partial C_L / \partial \alpha\right)_{\delta}}$

$c_{h_{\delta}}$ $\left(\partial c_{h_e} / \partial \delta\right)_{\alpha, \delta_t}$

$c_{h_{\alpha}}$ $\left(\partial c_{h_e} / \partial \alpha\right)_{\delta, \delta_t}$

The subscript outside the parenthesis indicates the factor held
constant in determining the parameter.

Subscripts:

LL   lifting-line theory

LLM   modified lifting-line theory

LS   lifting-surface theory

strip   strip

max   maximum

TE   trailing edge

e   elevator or effective

f   flap

δ   elevator-deflection-type load

α   angle-of-attack-type load

$\Delta\alpha_i$ incremental induced angle-of-attack-type load

i   induced

SC   streamline curvature

Angular measures are in radians in the text and in degrees in appendixes A and B and table I unless specified otherwise.

ELECTROMAGNETIC-ANALOGY MODEL

Lifting-line-theory vortex pattern.- The vortex pattern for an elliptic tail surface of aspect ratio 3 at zero angle of attack with a 0.5-chord 0.85-span elevator deflected is desired. In order to determine the vortex pattern, it is necessary to know the span load distribution as estimated from lifting-line theory and the chord load distribution as estimated from thin-airfoil theory.

The span load distribution for an elliptic wing having an aspect ratio of 3 and a section slope of the lift curve of 2π per radian and with 0.85-span elevator was determined quite accurately from unpublished influence lines similar to those of reference 8, but calculated for elliptic wings. The span load distribution, in terms of the parameter $\dfrac{c\alpha_e}{c_s\alpha}$, is given in figure 4.

The chordwise circulation function $\dfrac{2\Gamma}{cc_lV}$ must be known for both a flat plate at an angle of attack and a flat plate at zero angle of attack with a 0.5-chord elevator deflected. The mathematical expressions for these functions are given in references 3 and 9, and curves of the functions as estimated from thin-airfoil theory are presented in figure 5.

In order to construct the vortex pattern, it is necessary to determine how much of the load $\left(\dfrac{c\alpha_e}{c_s\alpha} \text{ of fig. 4}\right)$ at each section is elevator-type loading and how much is angle-of-attack-type loading. According to the assumptions of lifting-line theory, the amount of elevator-type loading is that given by strip theory; that is, this

loading is equal to the two-dimensional loading with aerodynamic induction neglected. The induced loading is entirely angle-of-attack-type loading and is equal to the loading obtained by strip theory minus the actual resultant loading given in figure 4.

The strip-theory loading over the elevator span in terms of the parameter $\dfrac{c\alpha_e}{c_s\alpha}$ is equal to $\dfrac{c}{c_s}$ (see fig. 4) since $\alpha_e = \alpha$ by definition. The circulation strength of elevator-type loading therefore is equal to $\left(\dfrac{2\Gamma}{cc_lV}\right)_\delta \dfrac{c}{c_s}$. The circulation strength of angle-of-attack-type loading is then equal to $\left(\dfrac{2\Gamma}{cc_lV}\right)_\alpha\left(\dfrac{c}{c_s} - \dfrac{c\alpha_e}{c_s\alpha}\right)$. If all values of circulation strength are divided by the maximum value at the wing center section, the values of Γ/Γ_{max} at any spanwise station $\dfrac{y}{b/2}$ and at any chordwise station x/c can be determined from figures 4 and 5 by the formulas that follow. For values of $\dfrac{y}{b/2}$ from 0 to 0.85,

$$\frac{\Gamma}{\Gamma_{max}} = \frac{\left(\dfrac{2\Gamma}{cc_lV}\right)_\delta \dfrac{c}{c_s} - \left(\dfrac{2\Gamma}{cc_lV}\right)_\alpha\left(\dfrac{c}{c_s} - \dfrac{c\alpha_e}{c_s\alpha}\right)}{\left(\dfrac{2\Gamma}{c_s c_l V}\right)_{max}} \tag{1a}$$

For values of $\dfrac{y}{b/2}$ from 0.85 to 1.0,

$$\frac{\Gamma}{\Gamma_{max}} = \frac{\left(\dfrac{2\Gamma}{cc_lV}\right)_\alpha\left(\dfrac{c\alpha_e}{c_s\alpha}\right)}{\left(\dfrac{2\Gamma}{c_s c_l V}\right)_{max}} \tag{1b}$$

Contour lines of $\dfrac{\Gamma}{\Gamma_{max}}$ determined from equations (1) for this configuration are given in figure 1.

Modified lifting-line-theory vortex pattern.- As stated in the "Introduction," it is desirable to fair the contour lines arbitrarily in the region just ahead of the elevator tip in order to simplify the construction of the model and to account approximately for the known smoothing effects of aerodynamic induction. The fairing over the region occupied by the elevator was not altered. The contour lines of figure 3 were obtained by fairing the curves of figure 1 similarly to the contour lines of figure 2. The contour lines of figure 3 were then used as the first approximation to the circulation strength (called modified lifting-line-theory loading).

Construction of Model

An electromagnetic-analogy model (fig. 6) of the loading represented by the contour lines of figure 3 was constructed and tested. The model was constructed of 100 wires representing the incremental vortices. The wires used were B. & S. No. 15 gage (0.057 in. diam.) copper. The span of the model was 100 inches, and the wake extended 2.4 semispans from the leading edge of the root section. The test setup, measuring equipment, and methods were similar to those described in reference 4.

LIFTING-SURFACE-THEORY CALCULATIONS FOR DOWNWASH

Because the additional lifting-surface-theory plan-form corrections are determined from the difference between the actual downwash measurements and the values estimated by lifting-line and thin-airfoil theories, it is necessary to calculate the downwash from these two-dimensional theories, as well as to measure the downwash for the electromagnetic-analogy model.

Downwash Calculated by Two-Dimensional Theories

Lifting-line-theory loading.- The downwash given by the 2 two-dimensional theories corresponding to the lifting-line-theory loading is, of course, equal to the geometric slope of the surface times the free-stream velocity. This value of downwash is everywhere zero except over the elevator itself. Over the elevator the downwash is equal to δV where

$$\delta = \frac{1}{(\alpha_\delta)_{c_l}} \frac{c_l}{c_{l_\alpha}} = \frac{c_l}{c_{l_\delta}}$$

and

$$c_l = \frac{2\Gamma_{strip}}{cV}$$

$$= \frac{2\Gamma_{TE}}{cV} \frac{\alpha}{\alpha_e}$$

and therefore

$$w_\delta = \delta V$$

$$= \frac{2\Gamma_{TE} \alpha}{\left(\alpha_\delta\right)_{c_l} c_{l_\alpha} \alpha_e c}$$

The downwash in terms of a nondimensional parameter is thus

$$\left(\frac{wb}{2\Gamma_{max}}\right)_\delta = \frac{2}{\dfrac{c}{b/2} \left(\dfrac{c\alpha_e}{c_s\alpha}\right)_{max} \left(\alpha_\delta\right)_{c_l} c_{l_\alpha}} \tag{2}$$

since

$$\Gamma_{max} = \Gamma_{TE}$$

and

$$\frac{c\alpha_e}{c_s\alpha} = \frac{\alpha_e}{\alpha}$$

where

$$c_s = c$$

From figure 4, $\left(\dfrac{c\alpha_e}{c_s\alpha}\right)_{max} = 0.59$; for a thin airfoil, $c_{l_\alpha} = 2\pi$;

for $\dfrac{c_e}{c} = 0.5$, $\left(\alpha_\delta\right)_{c_l} = \dfrac{\pi + 2}{2\pi}$; and for an elliptic wing of

$A = 3$, $\dfrac{c_s}{b/2} = \dfrac{8}{3\pi}$. The increment of downwash over the flap there-

fore is $\left(\dfrac{wb}{2\Gamma_{max}}\right)_\delta = 0.778$.

The downwash corresponding to the spanwise distribution of Γ_{TE} is just neutralized by the downwash corresponding to the bound vorticity of the induced load (of angle-of-attack type). This downwash must be calculated, however, in order to determine the modified lifting-line-theory downwash.

The downwash resulting from aerodynamic induction is equal to $\alpha_i V$ or $(\alpha - \alpha_e)V$. Over the sections of the model within the elevator span, $\alpha = \delta(\alpha_\delta)_{c_l}$; and over the section outboard of the elevator, $\alpha = 0$. For all sections

$$\alpha_e = \frac{2\Gamma_{TE}}{c_{l_\alpha} cV}$$

since

$$\Gamma_{TE} = \frac{cc_l V}{2} = \frac{c_{l_\alpha} \alpha_e cV}{2}$$

The induced downwash over the span of the elevator is thus

$$\left(\frac{wb}{2\Gamma_{max}}\right)_{i_{LL}} = \left(\frac{wb}{2\Gamma_{max}}\right)_\delta (\alpha_\delta)_{c_l} - \frac{1}{\pi\left(\dfrac{c}{b/2}\right)} \frac{\dfrac{c\alpha_e}{c_s\alpha}}{\left(\dfrac{c\alpha_e}{c_s\alpha}\right)_{max}} \qquad (3)$$

and over the sections outboard at the elevator is

$$\left(\frac{wb}{2\Gamma_{max}}\right)_{i_{LL}} = -\frac{1}{\pi\left(\dfrac{c}{b/2}\right)} \frac{\dfrac{c\alpha_e}{c_s\alpha}}{\left(\dfrac{c\alpha_e}{c_s\alpha}\right)_{max}}$$

$$= -\frac{A}{8\left(\dfrac{c}{c_s}\right)} \frac{\dfrac{c\alpha_e}{c_s\alpha}}{\left(\dfrac{c\alpha_e}{c_s\alpha}\right)_{max}} \qquad (4)$$

These downwash parameters are plotted in figure 7.

Modified lifting-line-theory loading.- The additional aspect-ratio corrections are determined from the difference between the measured lifting-surface-theory downwash and the downwash calculated from the two-dimensional theories for the modified lifting-line-theory loading. The downwash corresponding to the arbitrary fairing of the contour lines (fig. 3) must therefore be calculated by the two-dimensional theories. Because the span loading was not changed by the arbitrary fairing, the component of downwash corresponding to the spanwise distribution of Γ_{TE} (equations (3) and (4)) is unchanged. The chordwise distribution between the stations $\frac{y}{b/2} = 0.70$ and $\frac{y}{b/2} = 0.95$ was altered.

The procedure used in calculating the chordwise distribution of the downwash was to plot the magnitude of the altered contour lines against the chordwise position in a form similar to figure 5. The curve of Γ/Γ_{max} thus obtained can be integrated by means of the Biot-Savart law to obtain the downwash at any point x_0 as follows:

$$\frac{wb}{2\Gamma_{max}} = \frac{1}{2\pi} \int_{0}^{\frac{c}{b/2}} \frac{1}{\left(\frac{x}{b/2} - \frac{x_0}{b/2}\right)} \frac{d\left(\Gamma/\Gamma_{max}\right)}{d\frac{x}{b/2}} d\frac{x}{b/2} \qquad (5)$$

The curve of Γ/Γ_{max} was integrated by assuming that each small segment of the curve could be approximated satisfactorily by a parabola, a procedure similar to that presented in reference 3.

The sum of the downwash due to the bound vorticity Γ/Γ_{max} given by equation (5) and the downwash induced by the spanwise distribution of Γ_{TE} (equations (3) and (4)) gives the incremental downwash caused by modifying the contour lines of figure 1. The incremental values with the geometric downwash give the total modified lifting-line-theory downwash.

Values of nondimensional downwash for the first-approximation or modified lifting-line-theory loading are presented in figure 8. The downwash curves are rather irregular, as might be expected, since the fairing of the curve of Γ/Γ_{max} was done entirely arbitrarily and any slight errors in this curve show up to a very magnified scale in the downwash curves.

Downwash Measurements from Electromagnetic-Analogy Model

The magnetic-field strength of the electromagnetic-analogy model was measured at four or five vertical heights, 25 spanwise stations, and from 25 to 60 chordwise stations. A number of repeat tests were made to check the accuracy of the measurements, and satisfactory checks were obtained.

The measured data were faired, extrapolated to zero vertical height, and converted to the nondimensional downwash function $\left(\dfrac{wb}{2\Gamma_{max}}\right)_{LS}$ as discussed in reference 4. Corrections for the finite length of the trailing vortex sheet were calculated and applied as indicated in reference 4. The final curves of $\left(\dfrac{wb}{2\Gamma_{max}}\right)_{LS}$ for the two semispans were then averaged and are presented in figure 9.

Incremental Values of Downwash

In figure 10 are presented the incremental values of the nondimensional downwash $\Delta\left(\dfrac{wb}{2\Gamma_{max}}\right)_{LS}$ as determined by taking the difference between the lifting-surface-theory values of figure 9 and the values obtained by the two-dimensional theories for the modified lifting-line-theory loading of figure 8.

DEVELOPMENT OF ASPECT-RATIO CORRECTION FORMULA

General Procedure

The incremental lifting-surface-theory aspect-ratio corrections are determined by calculating the increments of chordwise and spanwise loadings that would result from a lifting surface shaped to correspond to the differences between the lifting-surface-theory downwash and the downwash determined from the two-dimensional theories, that is, the loadings of a lifting surface with shape given by letting the slope of the surface equal the downwash distribution of figure 10.

Because the incremental aspect-ratio corrections are reasonably small, approximate formulas are usually used to evaluate them. The methods and formulas usually used are given in reference 1 and include first-order compressibility corrections (reference 10). Some preliminary computations were made by more exact methods for the present case, in which the downwash near the elevator tip is so irregular. These preliminary computations indicated that the corrections would

not be given with satisfactory accuracy unless the actual chordwise variation in downwash was used. The following formulas are therefore developed by use of thin-airfoil-theory methods (references 11 and 12).

The following development of the aspect-ratio corrections was made by means of incompressible-flow relations. First-order compressibility corrections may be estimated by use of the linear perturbation theory of reference 10 as was done in reference 1.

<div style="text-align:center">Lift</div>

The incremental correction to the lift of an elliptic tail surface is

$$\Delta C_L = \frac{4}{\pi} \frac{A}{AE + 2} \frac{2\Gamma_{max}}{bV} \int_0^{1.0} \frac{\Delta c_l}{\frac{2\Gamma_{max}}{bV}} \frac{c}{c_s} \, d\left(\frac{y}{b/2}\right) \qquad (6)$$

where values of the parameter $\dfrac{\Delta c_l}{\frac{2\Gamma_{max}}{bV}}$ are obtained from the data

presented in figure 10 through the use of the relationship

$$\frac{\Delta c_l}{\frac{2\Gamma_{max}}{bV}} = 4 \int_0^{1.0} \Delta\left(\frac{wb}{2\Gamma_{max}}\right)_{LS} \sqrt{\frac{x/c}{1 - \frac{x}{c}}} \, d\frac{x}{c} \qquad (7)$$

derived from thin-airfoil theory. (See equation (25) of chapter IV of reference 11.)

Evaluation of $\left(\Delta C_{L\delta}\right)_{LS}$ requires an estimation of the relation between Γ_{max} and the elevator deflection δ. In accordance with lifting-line theory, $\left(\dfrac{c\alpha_e}{c_s\alpha}\right)_{max} = 0.59$. (See fig. 4 for this particular wing-flap combination.)

Thus,

$$\alpha_e = 0.59\alpha$$

$$\alpha_e = 0.59(\alpha_\delta)_{c_l}\,\delta$$

$$\alpha_e = 0.59\left(\frac{\pi + 2}{2\pi}\right)\delta$$

and

$$\Gamma_{max_{LL}} = \frac{c_s c_l V}{2} = \frac{c_s V}{2}\,2\pi\alpha_e = c_s V\delta(1.517) \tag{8}$$

In reference 1 are given values of the ratio $\left[\dfrac{(\alpha_\delta)_{c_L}}{(\alpha_\delta)_{c_l}}\right]_{LS}$
for full-span elevators. If the assumption is made that this correction is approximately proportional to the elevator span and if the Jones edge-velocity correction is applied, a more nearly correct relation between Γ_{max} and δ can be obtained from the following approximation:

$$\Gamma_{max} = \Gamma_{max_{LL}}\frac{A + 2}{AE + 2}\left(\left\{\left[\frac{(\alpha_\delta)_{c_L}}{(\alpha_\delta)_{c_l}}\right]_{LS} - 1\right\}\frac{b_e}{b} + 1\right) \tag{9}$$

or

$$\frac{2\Gamma_{max}}{bV} = \frac{1.517 \times 8}{A\pi}\frac{A + 2}{AE + 2}\left(\left\{\left[\frac{(\alpha_\delta)_{c_L}}{(\alpha_\delta)_{c_l}}\right]_{LS} - 1\right\}\frac{b_e}{b} + 1\right)\delta \tag{10}$$

and

$$\left(\Delta C_{L_\delta}\right)_{LS} = \frac{48.5}{\pi^2} \frac{A+2}{(AE+2)^2} \left(\left\{ \left[\frac{(\alpha_\delta)_{C_L}}{(\alpha_\delta)_{c_l}} \right]_{LS} - 1 \right\} \frac{b_e}{b} + 1 \right) \int_0^{1.0} \frac{\Delta c_l}{\frac{2\Gamma_{max}}{bV}} \frac{c}{c_s} d\left(\frac{y}{b/2}\right) \quad (11)$$

Therefore

$$\left(\Delta C_{L_\delta}\right)_{LS} = 0.855 \int_0^{1.0} \frac{\Delta c_l}{\frac{2\Gamma_{max}}{bV}} \frac{c}{c_s} d\left(\frac{y}{b/2}\right)$$

For the present case of a horizontal tail of aspect ratio 3, with a
0.5-chord 0.85-span plain elevator

$$\left(\Delta C_{L_\delta}\right)_{LS} = 0.855 \times 0.41$$

$$= 0.35 \qquad (12)$$

The lifting-line-theory value of C_{L_δ} for an elliptic wing
with a partial-span constant-percentage-chord elevator is given by

$$\left(C_{L_\delta}\right)_{LL} = \frac{8A(\alpha_\delta)_{c_l} \int_0^{b_e/b} \frac{c}{c_s} d\left(\frac{y}{b/2}\right)}{A+2} \qquad (13)$$

for a lift-curve slope of 2π.

For the wing under discussion with a value of $(\alpha_\delta)_{c_l}$ of $\frac{\pi+2}{2\pi}$

$$\left(C_{L_\delta}\right)_{LL} = 2.87$$

and

$$\left(C_{L_\delta}\right)_{LS} = \left(C_{L_\delta}\right)_{LL} - \left(\Delta C_{L_\delta}\right)_{LS} = 2.52$$

If it is assumed that the concept of an effective edge-velocity correction (see reference 1) can be used in the partial-span-flap case, then

$$\left(C_{L_\delta}\right)_{LS} = \frac{0.93 \times 2\pi\left(\alpha_\delta\right)_{c_l} A}{AE_{e_f} + 2} = \frac{0.93(\pi + 2)A}{AE_{e_f} + 2} = 2.52$$

which gives for E_{e_f} a value of 1.23. Thus, for section slopes of the lift curve not equal to 2π, the following assumption may be made:

$$\left(C_{L_\delta}\right)_{LS} = \frac{0.93 c_{l_\alpha}\left(\alpha_\delta\right)_{c_l}}{E_{e_f} + \dfrac{c_{l_\alpha}}{\pi A}} \tag{14}$$

Hinge Moment

Determination of $\left(C_{h_\delta}\right)_{LS}$.- The lifting-surface-theory hinge-moment parameter $\left(C_{h_\delta}\right)_{LS}$ is given by the expression

$$\left(C_{h_\delta}\right)_{LS} = \left(C_{h_\delta}\right)_{LL} + \left(\Delta C_{h_\delta}\right)_{LS} \tag{15}$$

Because the contour lines over the elevator were not altered from those computed for the lifting-line-theory load, the lifting-line-theory value of the hinge-moment coefficient for the modified load is identical with that for the unmodified load. This value is

$$\left(C_{h_\delta}\right)_{LL} = c_{h_\delta} - c_{h_\alpha} \frac{\left(c_e/c\right)^2}{\left(\bar{c}_e/c_s\right)^2 \dfrac{b_e}{b}} \int_0^{b_e/b} \left[\frac{\left(\dfrac{vb}{2\Gamma_{max}}\right)_{iLL}}{0.778}\right]_{LL} \left(\frac{c}{c_s}\right)^2 d\left(\frac{y}{b/2}\right) \tag{16}$$

From the wing geometry

$$\frac{\left(c_e/c\right)^2}{\left(\bar{c}_e/c_s\right)^2 \dfrac{b_e}{b}} = 1.55$$

From the downwash curves of figure 7 the integral may be evaluated as 0.2215. This evaluation assumes the span-load curve to be unchanged by small changes in the slope of the lift curve. Equation (15) may be written as

$$\left(c_{h_\delta}\right)_{LS} = c_{h_\delta} - 0.344 c_{h_\alpha} + \left(\Delta c_{h_\delta}\right)_{LS} \tag{17}$$

The lifting-surface-theory correction to the slope of the hinge moment against elevator deflection $\left(\Delta c_{h_\delta}\right)_{LS}$ is equal to the hinge moment of a 50-percent-chord elevator on a surface, which is given by the difference in the measured downwash and the lifting-line-theory downwash (fig. 10). Over most of the wing, the difference in downwash is equivalent to a parabolic-arc-camber airfoil at an angle of attack.

The hinge-moment corrections are computed by thin-airfoil-theory formula in two parts (see reference 1) as follows:

$$\left(\Delta c_{h_\delta}\right)_{LS} = \left(\Delta c_{h_\delta}\right)_{\Delta\alpha_i} + \left(\Delta c_{h_\delta}\right)_{SC} \tag{18}$$

The increment $\left(\Delta c_{h_\delta}\right)_{\Delta\alpha_i}$ is obtained from the induced downwash at the 0.5-chord point. The increment $\left(\Delta c_{h_\delta}\right)_{SC}$ is not a streamline-curvature correction in the sense used in reference 1, since the downwash curves near the outboard end of the flap define a somewhat irregular surface, not a parabolic-arc surface. The hinge-moment corrections estimated by the two methods, although appreciable, are not too great; therefore, for the purpose of simplifying the system of notation and in order that the viscosity efficiency factor η for parabolic-arc airfoils can be used for the present case, the symbol $\left(\Delta c_{h_\delta}\right)_{SC}$ is used to

identify the part of the correction not given by $\left(\Delta c_{h\delta}\right)_{\Delta\alpha_i}$. The numerical values of $\left(\Delta c_{h\delta}\right)_{SC}$

are computed, however, for the actual distorted surface.

The induced-angle-of-attack correction is

$$\left(\Delta c_{h\delta}\right)_{\Delta\alpha_i} = -c_{h\alpha}\frac{A}{AE + 2}\frac{\left(c_e/c\right)^2}{\dfrac{b_e}{b}\left(\bar{c}_e/c_s\right)^2}\int_0^{b_e/b}\frac{\Delta\alpha_i}{\delta}\left(\frac{c}{c_s}\right)^2 d\left(\frac{y}{b/2}\right) \tag{19}$$

If the value of $\Delta\alpha_i$ is given in terms of the increment of downwash parameter at the

c/2 stations $\Delta\left(\dfrac{vb}{2\Gamma_{max}}\right)_{c/2}\dfrac{2\Gamma_{max}}{bV}$ and the value of δ is obtained from equation (10), the

following equation is obtained:

$$\left(\Delta c_{h\delta}\right)_{\Delta\alpha_i} = -c_{h\alpha}\frac{\left(c_e/c\right)^2}{\dfrac{b_e}{b}\left(\bar{c}_e/c_s\right)^2}\,3.86\,\frac{A + 2}{\left(AE + 2\right)^2}\left\{\left[\frac{(\alpha_\delta)_{C_L}}{(\alpha_\delta)_{c_l}} - 1\right]\frac{b_e}{b} + 1\right\}\int_0^{b_e/b}\Delta\left(\frac{vb}{2\Gamma_{max}}\right)_{c/2}\left(\frac{c}{c_s}\right)^2 d\left(\frac{y}{b/2}\right) \tag{20}$$

By the use of the data of figure 10 the integral was evaluated; hence

$$\left(\Delta c_{h\delta}\right)_{\Delta\alpha_i} = -0.017 c_{h\alpha} \tag{21}$$

The value of $\left(\Delta c_{h\delta}\right)_{SC}$ may be determined from

$$\left(\Delta c_{h\delta}\right)_{SC} = \frac{2\Gamma_{max}}{bV\delta}\frac{\left(\frac{c_e}{c}\right)^2}{\frac{b_e}{b}\left(\frac{\overline{c}_e}{c_s}\right)^2}\int_0^{b_e/b}\frac{\Delta c_h}{2\Gamma_{max}/bV}\left(\frac{c}{c_s}\right)^2 d\left(\frac{y}{b/2}\right) \tag{22}$$

where values of the parameter $\dfrac{\Delta c_h}{2\Gamma_{max}/bV}$ are obtained from the data presented in figure 9 by means of the relation

$$\frac{\Delta c_h}{\frac{2\Gamma_{max}}{bV}} = \int\left(\frac{\partial c_h}{\partial\delta_t}\right)_{\alpha_o,\delta} d\left[\Delta\left(\frac{wb}{2\Gamma_{max}}\right) - \Delta\left(\frac{wb}{2\Gamma_{max}}\right)_{0.5c}\right] \tag{23}$$

Numerical values of the parameter $\left(\dfrac{\partial c_h}{\partial\delta_t}\right)_{\alpha_o,\delta}$ are presented in figure 11 for a 0.5-chord plain elevator as calculated from the thin-airfoil-theory formulas of reference 12. For flaps with overhang or internal balances, the changes in the parabolic-arc factor $\dfrac{F}{\left(c_e/c\right)^2}$ of reference 1 with the amount of balance can be used as a fair measure of the changes with overhang of the value of $\left(\Delta c_{h\delta}\right)_{SC}$ determined from equations (22) and (23).

For a horizontal tail surface of aspect ratio 3, with 0.5-chord 0.85-span plain elevator having an assumed value of $c_{l_\alpha} = 2\pi$

and $\left(\alpha_\delta\right)_{c_l} = \dfrac{\pi+2}{2\pi}$

$$\left(\Delta C_{h\delta}\right)_{SC} = 0.2005 \quad \text{per radian} \tag{24}$$

The lifting-surface-theory value of the parameter $\left(C_{h\delta}\right)_{LS}$ is obtained by substitution of values from equations (18), (21), and (24) in equation (17) as follows:

$$\left(C_{h\delta}\right)_{LS} = c_{h\delta} - 0.361c_{h\alpha} + 0.2005$$

In order to estimate $\left(C_{h\delta}\right)_{LS}$ for the plan-form corrections from the section data with arbitrary values of $c_{l\alpha}$, $\left(\alpha_\delta\right)_{c_l}$, $c_{h\alpha}$, and $c_{h\delta}$ the following expression may be used:

$$\left(c_{h\delta}\right)_{LS} = c_{h\delta} - \frac{1.1\left(\alpha_\delta\right)_{c_l}}{1 + \dfrac{3\pi}{c_{l\alpha}}} c_{h\alpha} - 0.0487 \frac{F\eta}{\left(c_e/c\right)^2} \frac{\left(\alpha_\delta\right)_{c_l} c_{l\alpha}}{1 + \dfrac{c_{l\alpha}}{3\pi}} \tag{25}$$

where $A = 3$, $\eta = 1 - 0.0005 \, \phi^2$, and values of $\dfrac{F}{\left(c_e/c\right)^2}$ are presented in reference 1.

Determination of $\left(C_{h\alpha}\right)_{LS}$.- The lifting-surface-theory hinge-moment parameter $\left(C_{h\alpha}\right)_{LS}$ for an elliptic tail surface with a partial-span constant-percentage-chord elevator may be estimated from the relation

$$\left(C_{h\alpha}\right)_{LS} = c_{h\alpha} \left(1 - \frac{\alpha_i}{\alpha}\right)_{LS} + \frac{\left[\left(\Delta C_{h\alpha}\right)_{SC}\right]_{\text{Partial-span}}}{\left[\left(\Delta C_{h\alpha}\right)_{SC}\right]_{\text{Full-span}}} \left[\left(\Delta C_{h\alpha}\right)_{SC}\right]_{\text{Full-span}}$$

Γ

Values of $\left[\left(\Delta C_{h_\alpha}\right)_{SC}\right]_{\text{Full-span}}$ and $\left(\dfrac{\alpha_1}{\alpha}\right)_{LS}$ are presented in

reference 1 and values of the ratio $\dfrac{\left[\left(\Delta C_{h_\alpha}\right)_{SC}\right]_{\text{Partial-span}}}{\left[\left(\Delta C_{h_\alpha}\right)_{SC}\right]_{\text{Full-span}}}$, derived

from the curves used in estimating the corrections presented in
reference 2, are given in figure 12.

COMPARISON OF LIFTING-SURFACE-THEORY RESULTS

WITH WIND-TUNNEL DATA

The difference between the aspect-ratio corrections for full-
span elevators and partial-span elevators can be determined from
the wind-tunnel data presented in appendix A for a condition
directly comparable to the case considered in the present paper
($A = 3$, elliptic plan form, $\dfrac{c_e}{c} = 0.5$, and $\dfrac{b_e}{b} = 0.85$). In

reference 1, some difficulty was encountered in checking the
accuracy of the theoretical aspect-ratio corrections against
experimental wind-tunnel data because of the scarcity of comparable
section and finite-span data. Even the slight surface irregu-
larities obtained in construction of two different models caused
large enough changes in the measured hinge moments so that the
accuracy of the theoretical aspect-ratio corrections was difficult
to evaluate. The accuracy of checking the difference in the
corrections for the full-span elevator and the partial-span ele-
vator, however, should be relatively good since the same model
was used for both tests, the tip of the elevator being fastened
to the elevator in one case and to the stabilizer in the other
case.

In table I is presented a summary of the lift and hinge-
moment parameters measured from the wind-tunnel data of figure 13
and estimated by means of lifting-line and lifting-surface theories.
No values were estimated for the elevator with cut-out. In
table II the incremental differences in the parameters for the
full-span and the partial-span elevator are given, and in table III
the lift and hinge-moment parameters caused by cut-out are given.
For the lift parameters both theories predicted approximately the
correct increment; however, the slope of the hinge-moment coeffi-
cient against elevator deflection estimated by lifting-surface

theory is in much better agreement with the experimental values than the slopes estimated by lifting-line theory.

Only about 10 percent of the incremental difference for the slope of the curve of hinge-moment coefficient against elevator deflection is given by lifting-line theory; the total lifting-surface-theory increment is -0.0009 per degree for the configuration considered herein.

The effects of the cut-out, especially upon the hinge-moment characteristics, were extremely large (see table I) and no adequate theory is available to estimate the effects of the cut-out. In addition, very little experimental section data are available for airfoil sections similar to those at the cut-out. The large effect of the cut-out indicates that lifting-surface-theory solutions such as are given in the present paper and in reference 1 are definitely limited to tail surfaces without cut-outs as well as to small angles of attack and small elevator deflections.

CONCLUDING REMARKS

An electromagnetic-analogy model of the vortex load, estimated from lifting-line theory with an arbitrary fairing near the elevator tip, on a thin elliptic horizontal tail surface of aspect ratio 3 with a 0.5-chord 0.85-span plain elevator was constructed and tested. The aspect-ratio corrections to the lift and hinge moments were calculated from the measured results.

A comparison of the aspect-ratio corrections for the partial-span elevators was made with those previously presented for full-span elevators. The comparison indicates that the incremental difference in the lift parameters between the full-span and the partial-span elevators may be estimated satisfactorily by lifting-line theory. The incremental difference for the curve of hinge-moment coefficient against angle of attack is usually small. Only about 10 percent of the incremental difference for the slope of the curve of hinge-moment coefficient against elevator deflection is given by lifting-line theory; the total lifting-surface-theory increment is -0.0009 per degree for the configuration considered herein.

Wind-tunnel results for a tail surface of the same plan form were presented. The differences in the estimated lifting-surface aspect-ratio corrections for the full-span and partial-span elevators were checked satisfactorily by the experimental data. A few tests with a cut-out for the rudder were also presented. The

effects of the cut-out, especially upon the hinge-moment character-
istics, were extremely large and no adequate theory is available
to estimate the effects of the cut-out. The large effect of the
cut-out indicates that lifting-surface-theory solutions such as
are given in the present paper and previously are definitely limited
to tail surfaces without cut-outs as well as to small angles of
attack and small elevator deflections.

Langley Memorial Aeronautical Laboratory
    National Advisory Committee for Aeronautics
        Langley Field, Va., August 20, 1946

APPENDIX A

WIND-TUNNEL TESTS

By E. Page Hoggard, Jr.

The test results presented herein were obtained to check the
theoretical changes in the aspect-ratio corrections resulting from
the use of partial-span elevators. The effect of a rudder cut-out
in the elevator was also tested to find out the order of magnitude
of such a modification of the elevator.

Apparatus, Model, Corrections, and Tests

All tests were made in the Langley 4- by 6-foot vertical
tunnel modified as described in reference 13. The elliptic semispan
tail surface (fig. 14) was constructed of laminated mahogany and
conformed to the NACA 0009 profile. In the present investigation
one elevator with a chord 50 percent of the tail chord was tested.
This elevator had a plain radius nose with a gap of 0.5 percent of
the airfoil chord. The model was equipped with a removable cut-out
block and an elevator tip block so that the four model configurations
shown in figure 14 could be obtained. The elevator tip block could
be fastened to the elevator or to the main part of the tail surface.
The trailing-edge angle of the model measures 11.1°, whereas the
theoretical trailing-edge angle (from the published ordinates)
measures 11.6° for the NACA 0009 airfoil.

The tail surface was installed as a reflection-plane model
by mounting the model with the root section adjacent to one of the
tunnel walls. This system is therefore analogous to mounting a
6-foot-span model in an 8- by 6-foot tunnel. The model was
supported by the balance frame so that the lift acting on the
model could be measured. The gap between the tunnel wall and the
root section was about 1/32 inch.

The greater part of the elevator hinge moment (transmitted
through a torque tube) was measured by applying weights at a known
lever arm outside the tunnel; the additional increment was measured
with a calibrated dial attached to a long flexible torque rod.

Elevator deflections were set with an electric control-surface
position indicator.

Each model configuration was tested with the gap open and with the gap sealed. The seal was made of impregnated fabric. The model was tested through an angle-of-attack range of $\pm 20°$ with elevator neutral, and at zero angle of attack through an elevator-deflection range from $-5°$ to $30°$.

A dynamic pressure of 13 pounds per square foot, which corresponds to an airspeed of 71 miles per hour at standard sea-level conditions, was maintained for all tests. The test Reynolds number was 1.43×10^6 based on a mean aerodynamic chord of 25.81 inches. The effective Reynolds number (for maximum lift coefficients) was approximately 2.76×10^6 based on a turbulence factor of 1.93 for this tunnel.

No correction was made for leakage around the model support. The following tunnel-wall corrections were added to the data:

$$\Delta\alpha = 2.184 \, C_{L_T} \quad \text{(for all four model configurations)}$$

$$\Delta C_h = 0.0134 \, C_{L_T} \quad \text{(full-span elevator without cut-out)}$$

$$\Delta C_h = 0.0135 \, C_{L_T} \quad \text{(full-span elevator with cut-out)}$$

$$\Delta C_h = 0.0159 \, C_{L_T} \quad \text{(partial-span elevator without cut-out)}$$

$$\Delta C_h = 0.0163 \, C_{L_T} \quad \text{(partial-span elevator with cut-out)}$$

where C_{L_T} is the total uncorrected lift coefficient. For methods of calculating corrections for reflection-plane models, see reference 14.

Although the elevator-deflection tests were run with the geometric angle of attack at zero, the jet-boundary correction $\Delta\alpha$ given in the foregoing corrections indicates that part of the total lift and elevator hinge moment results from a jet-boundary induced angle of attack. The plots against elevator deflection therefore were made and the slopes were read by using the test data as corrected in the following equations:

$$C_{L_{corrected}} = C_{L_{uncorrected}} - \Delta\alpha \, C_{L_\alpha}$$

$$C_{h_{corrected}} = C_{h_{uncorrected}} - \Delta\alpha \, C_{h_\alpha}$$

$$\left(\alpha_\delta\right)_{c_{l_{corrected}}} = \frac{C_{L_{\delta_{corrected}}}}{C_{L_\alpha}}$$

Data

The lift and elevator hinge-moment characteristics of the model tested are presented in figure 13. The various parameters are presented in table I. The slopes were determined for the small angle-of-attack and deflection range.

APPENDIX B

ESTIMATION OF C_{h_α} AND C_{h_δ} FOR FEELER AILERONS

Because the aspect-ratio corrections given in the present paper and in reference 1 are obtained from a linear lifting-surface theory, it is possible to superimpose the lifting-surface-theory solutions and thus obtain the solution for 0.5-chord 0.15-span feeler ailerons on a wing of aspect ratio 3. Of course, the arrangement obtained by the use of superposition simulates two ailerons, one on each wing tip, deflected in the same way. A few calculations indicate that the mutual influence of the ailerons upon the hinge-moment characteristics may, however, be safely neglected.

Detailed calculations of the aspect-ratio corrections for this arrangement are not presented because the procedure is similar to that used for the partial-span elevators as given in the main part of the paper.

Because the data are for a rather low aspect ratio for a wing $(A = 3)$, the results for the feeler aileron are mainly of comparative value. The incremental difference between the estimated finite-span values and the section values of the hinge-moment parameters (per degree) for the full-span elevator, the 0.85-span elevator, and the 0.15-span feeler aileron are as follows:

Configuration	ΔC_{h_α}	ΔC_{h_δ}
Full-span elevator	0.0060	0.0053
0.85-span elevator	.0059	.0062
0.15-span feeler aileron	.0104	.0090

where the section values are

$$c_{h_\delta} = -0.014$$

and

$$c_{h_\alpha} = -0.0104$$

The aspect-ratio corrections for the case of the feeler aileron are about 70-percent larger than for the case of the full-span elevator. The rather large values of the aspect-ratio corrections are shown especially for the aspect-ratio correction to C_{h_α}, which is equal to the section value, so that the net value of C_{h_α} equals 0.

REFERENCES

1. Swanson, Robert S., and Crandall, Stewart M.: Lifting-Surface-Theory Aspect-Ratio Corrections to the Lift and Hinge-Moment Parameters for Full-Span Elevators on Horizontal Tail Surfaces. NACA TN No. 1175, ~~1946.~~ *1947*

2. Swanson, Robert S., and Gillis, Clarence L.: Limitations of Lifting-Line Theory for Estimation of Aileron Hinge-Moment Characteristics. NACA CB No. 3L02, 1943.

3. Cohen, Doris: A Method for Determining the Camber and Twist of a Surface to Support a Given Distribution of Lift. NACA TN No. 855, 1942.

4. Swanson, Robert S., and Crandall, Stewart M.: An Electromagnetic-Analogy Method of Solving Lifting-Surface-Theory Problems. NACA ARR No. L5D23, 1945.

5. Wenzinger, Carl J., and Harris, Thomas A.: Pressure Distribution over a Rectangular Airfoil with a Partial-Span Split Flap. NACA Rep. No. 571, 1936.

6. Allen, H. Julian: Calculation of the Chordwise Load Distribution over Airfoil Sections with Plain, Split, or Serially Hinged Trailing-Edge Flaps. NACA Rep. No. 634, 1938.

7. Jones, Robert T.: Theoretical Correction for the Lift of Elliptic Wings. Jour. Aero. Sci., vol. 9, no. 1, Nov. 1941, pp. 8-10.

8. Pearson, Henry A., and Jones, Robert T.: Theoretical Stability and Control Characteristics of Wings with Various Amounts of Taper and Twist. NACA Rep. No. 635, 1938.

9. Crandall, Stewart M.: Lifting-Surface-Theory Results for Thin Elliptic Wings of Aspect Ratio 3 with Chordwise Loadings Corresponding to 0.5-Chord Plain Flap and to Parabolic-Arc Camber. NACA TN No. 1064, 1946.

10. Goldstein, S., and Young, A. D.: The Linear Perturbation Theory of Compressible Flow, with Applications to Wind-Tunnel Interference. R.&M. No. 1909, British A.R.C., 1943.

11. Munk, Max M.: Fundamentals of Fluid Dynamics for Aircraft Designers. The Ronald Press Co., 1929.

12. Theodorsen, Theodore, and Garrick, I. E.: Nonstationary Flow
       about a Wing-Aileron-Tab Combination Including Aerodynamic
       Balance.   NACA Rep. No. 736, 1942.

13. Ames, Milton B., Jr., and Sears, Richard I.: Pressure-Distribution
       Investigation of an N.A.C.A. 0009 Airfoil with a 30-Percent-
       Chord Plain Flap and Three Tabs.   NACA TN No. 759, 1940.

14. Swanson, Robert S., and Toll, Thomas A.: Jet-Boundary Correc-
       tions for Reflection-Plane Models in Rectangular Wind Tunnels.
       NACA ARR No. 3E22, 1943.

T

TABLE I

PARAMETERS MEASURED FROM WIND-TUNNEL DATA AND CALCULATED FROM THEORETICAL DATA

[Calculations were not made for the arrangements with cut-out because of a
lack of comparable section data and theoretical results.]

Lift

Gap	Cut-out	c_{L_α}						c_{L_δ}					
		Full-span flap			Partial-span flap			Full-span flap			Partial-span flap		
		Measured	Calculated		Measured	Calculated		Measured	Calculated		Measured	Calculated	
			(a)	(b)		(a)	(b)		(a)	(b)		(a)	(b)
Sealed	Without	0.052	0.062	0.053	0.052	0.062	0.053	0.041	0.048	0.042	0.038	0.045	0.040
0.005c	Without	.050	.060	.052	--------	.060	.052	.038	.046	.040	.036	.043	.038
Sealed	With	.049	-------	-------	.047	-------	-------	.031	-------	-------	.028	-------	-------
0.005c	With	.048	-------	-------	.048	-------	-------	.026	-------	-------	.023	-------	-------

Hinge-moment

Gap	Cut-out	c_{h_α}						c_{h_δ}					
		Full-span flap			Partial-span flap			Full-span flap			Partial-span flap		
		Measured	Calculated		Measured	Calculated		Measured	Calculated		Measured	Calculated	
			(a)	(b)		(a)	(b)		(a)	(b)		(a)	(b)
Sealed	Without	-0.0037	-0.0065	-0.0044	-0.0037	-0.0065	-0.0046	-0.0082	-0.0109	-0.0087	-0.0073	-0.0108	-0.0078
0.005c	Without	-.0043	-.0066	-.0045	-.0042	-.0066	-.0047	-.0078	-.0111	-.0090	-.0068	-.0109	-.0080
Sealed	With	-.0015	-------	-------	-.0013	-------	-------	-.0041	-------	-------	-.0038	-------	-------
0.005c	With	-.0019	-------	-------	-.0015	-------	-------	-.0056	-------	-------	-.0052	-------	-------

[a] Computed by lifting-line theory.
[b] Computed by lifting-surface theory.

NATIONAL ADVISORY
COMMITTEE FOR AERONAUTICS

TABLE II

INCREMENTS IN PARAMETERS CAUSED BY PARTIAL SPAN

Gap	Cut-out	$\Delta^{s}C_{L_\alpha}$			$\Delta^{s}C_{L_\delta}$			$\Delta^{s}C_{h_\alpha}$			$\Delta^{s}C_{h_\delta}$		
		Measured	Calculated		Measured	Calculated		Measured	Calculated		Measured	Calculated	
			(a)	(b)		(a)	(b)		(a)	(b)		(a)	(b)
Sealed	Without	0	0	0	0.003	0.003	0.002	0	0	0.0002	-0.0009	-0.0001	-0.0009
0.005c	Without	0	0	0	.003	.003	.003	-0.0001	0	.0002	-.0010	-.0002	-.0010
Sealed	With	0.002	----	----	.003	-----	-----	-.0002	---	------	-.0003	-------	-------
0.005c	With	0	----	----	.003	-----	-----	-.0004	---	------	-.0004	-------	-------

[a]Computed by lifting-line theory.

[b]Computed by lifting-surface theory.

TABLE III

INCREMENTS IN PARAMETERS CAUSED BY CUT-OUT

Gap	Flap span	$\Delta^{w}C_{L_\alpha}$	$\Delta^{w}C_{L_\delta}$	$\Delta^{w}C_{h_\alpha}$	$\Delta^{w}C_{h_\delta}$
Sealed	Full	0.003	0.010	-0.0022	-0.0041
0.005c	Full	.002	.012	-.0025	-.0022
Sealed	Partial	.005	.010	-.0021	-.0035
0.005c	Partial	-----	.012	-.0026	-.0016

NATIONAL ADVISORY
COMMITTEE FOR AERONAUTICS
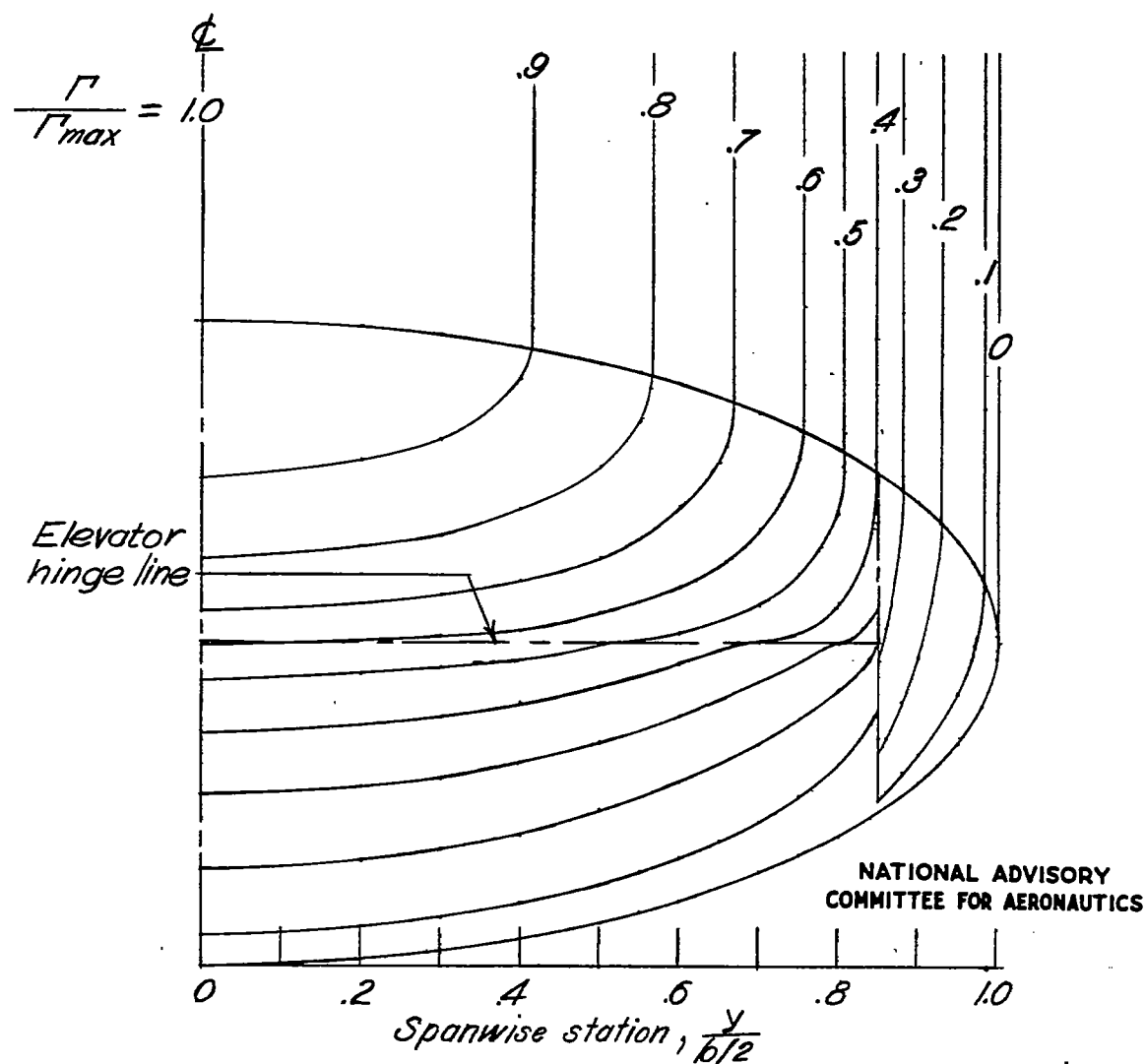
Figure 1.— Contour lines of the circulation function $\frac{\Gamma}{\Gamma_{max}}$ as estimated from thin-airfoil and lifting-line theories for an elliptic wing of aspect ratio 3 with a 0.5-chord 0.85-span plain elevator.

Fig. 2   NACA TN No. 1275
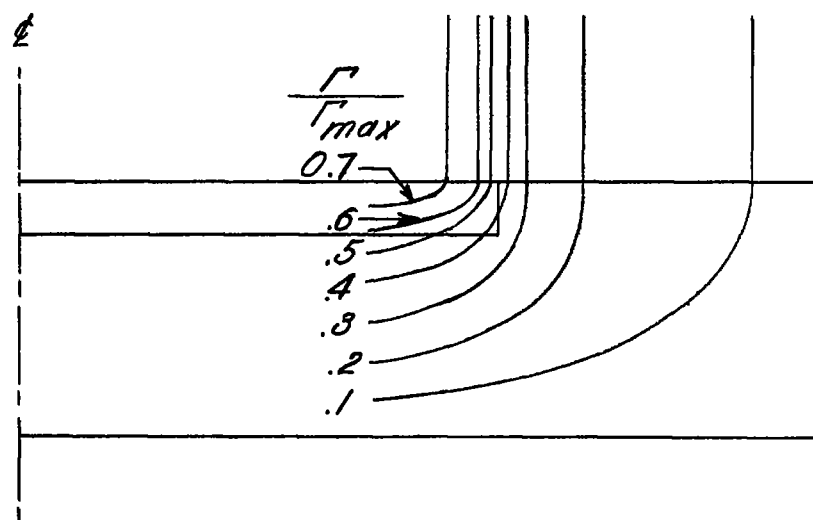
(a) Experimental values from integration of pressure distributions of reference 5.

Spanwise station, $\frac{y}{b/2}$
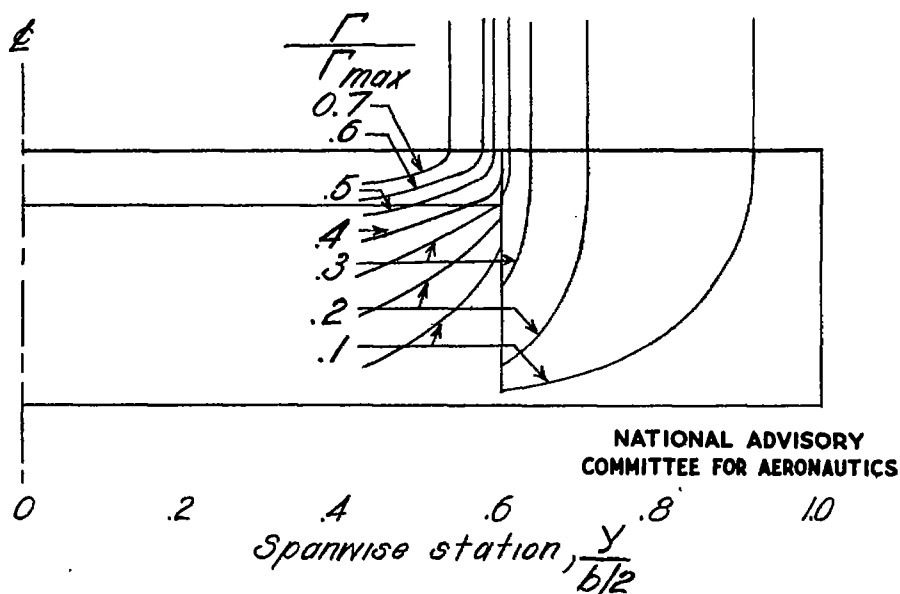
(b) Contour lines computed from the experimental span loading of reference 5 and divided into the experimental chord loadings of reference 6 by means of the assumptions of lifting-line theory.

Figure 2. — Contour lines of the circulation function $\frac{\Gamma}{\Gamma_{max}}$ for a rectangular wing with part-span split flaps. A = 6; $\frac{b_f}{b} = 0.6$; $\frac{c_f}{c} = 0.2$.
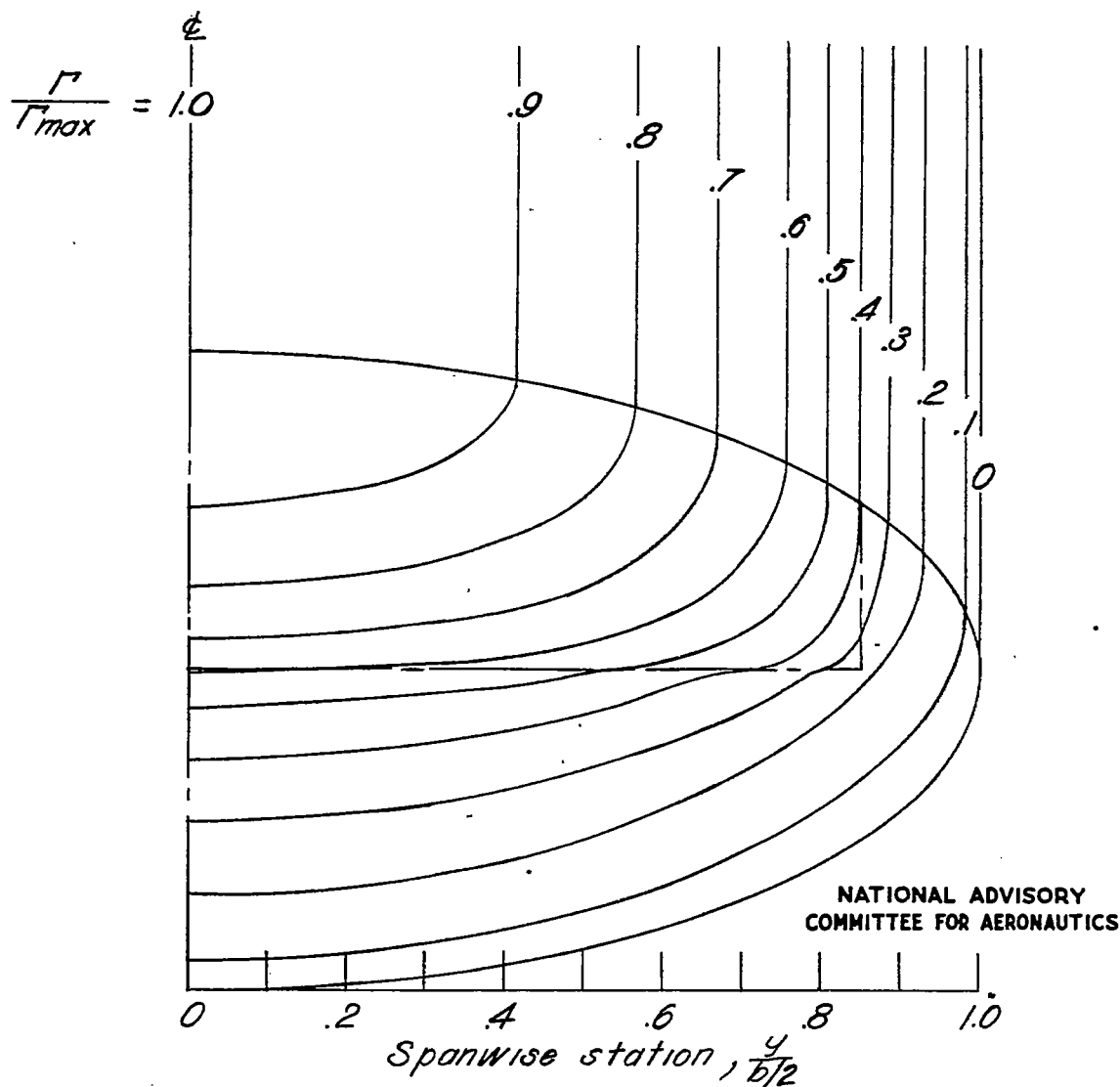
Figure 3 .- Contour lines of the circulation function $\frac{\Gamma}{\Gamma_{max}}$ used in constructing an electromagnetic-analogy model of an elliptic wing of aspect ratio 3 with a 0.5-chord 0.85-span elevator. Contour lines are same as those of figure 1 from $0 < \frac{y}{b/2} < 0.7$ with an arbitrary fairing from $0.7 < \frac{y}{b/2} < 1.0$.

Fig. 4
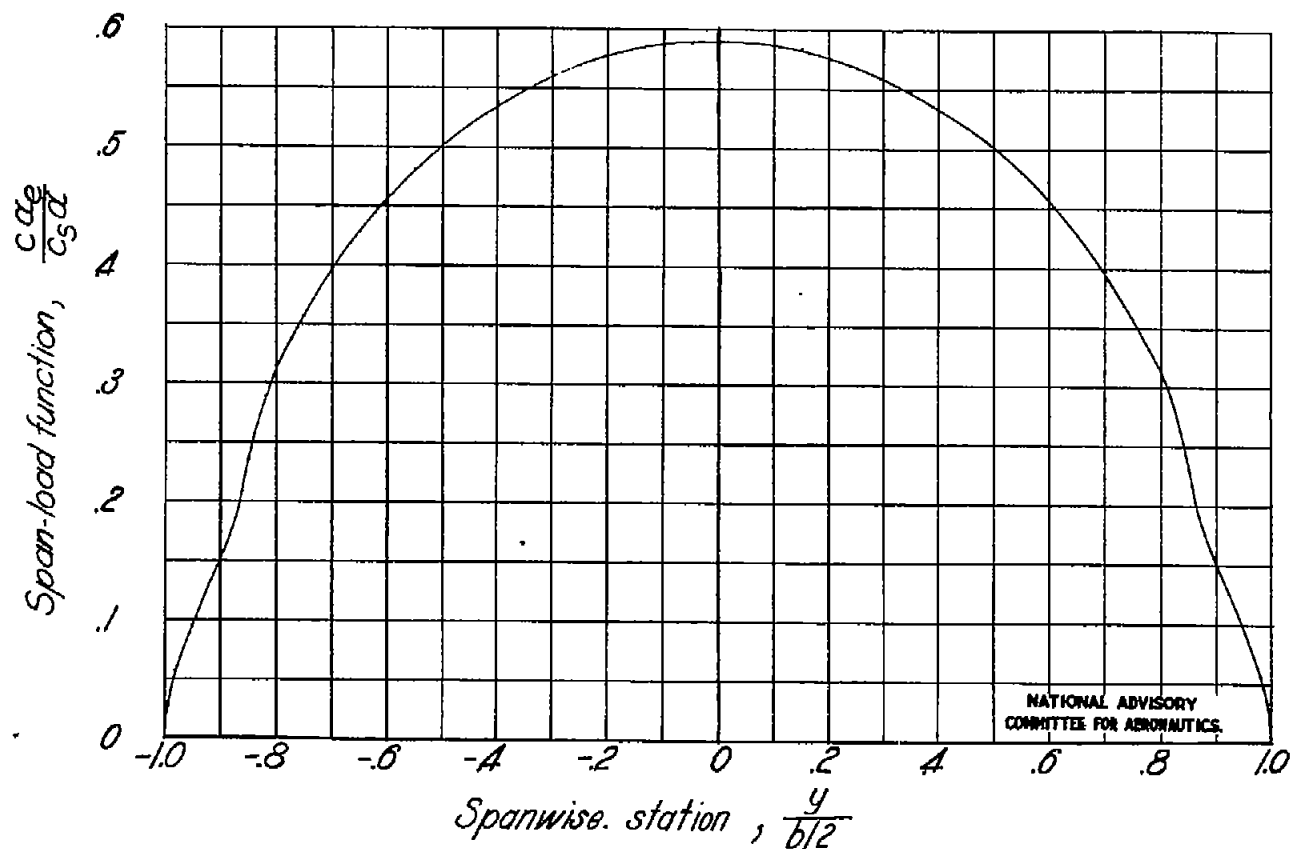
Figure 4.— Spanwise distribution of the span-load function $\frac{c\alpha_e}{c_s\alpha}$ for an elliptic wing of aspect ratio 3, with an 0.85-span flap as estimated from lifting-line theory. $a_0 = 2\pi$.
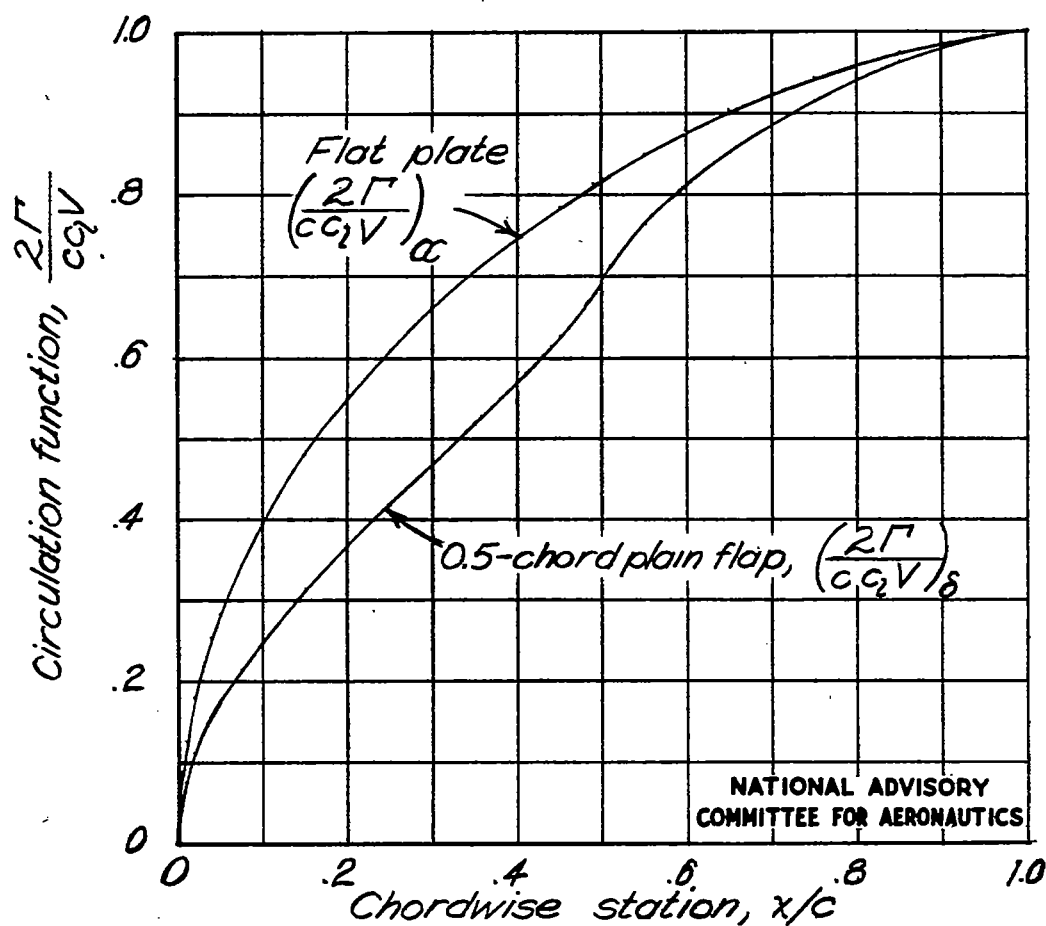
Figure 5 . — Chordwise distribution of the circulation function $\frac{2\Gamma}{c\,c_l V}$ for a flat plate and for a 0.5-chord plain flap as estimated from thin-airfoil theory .
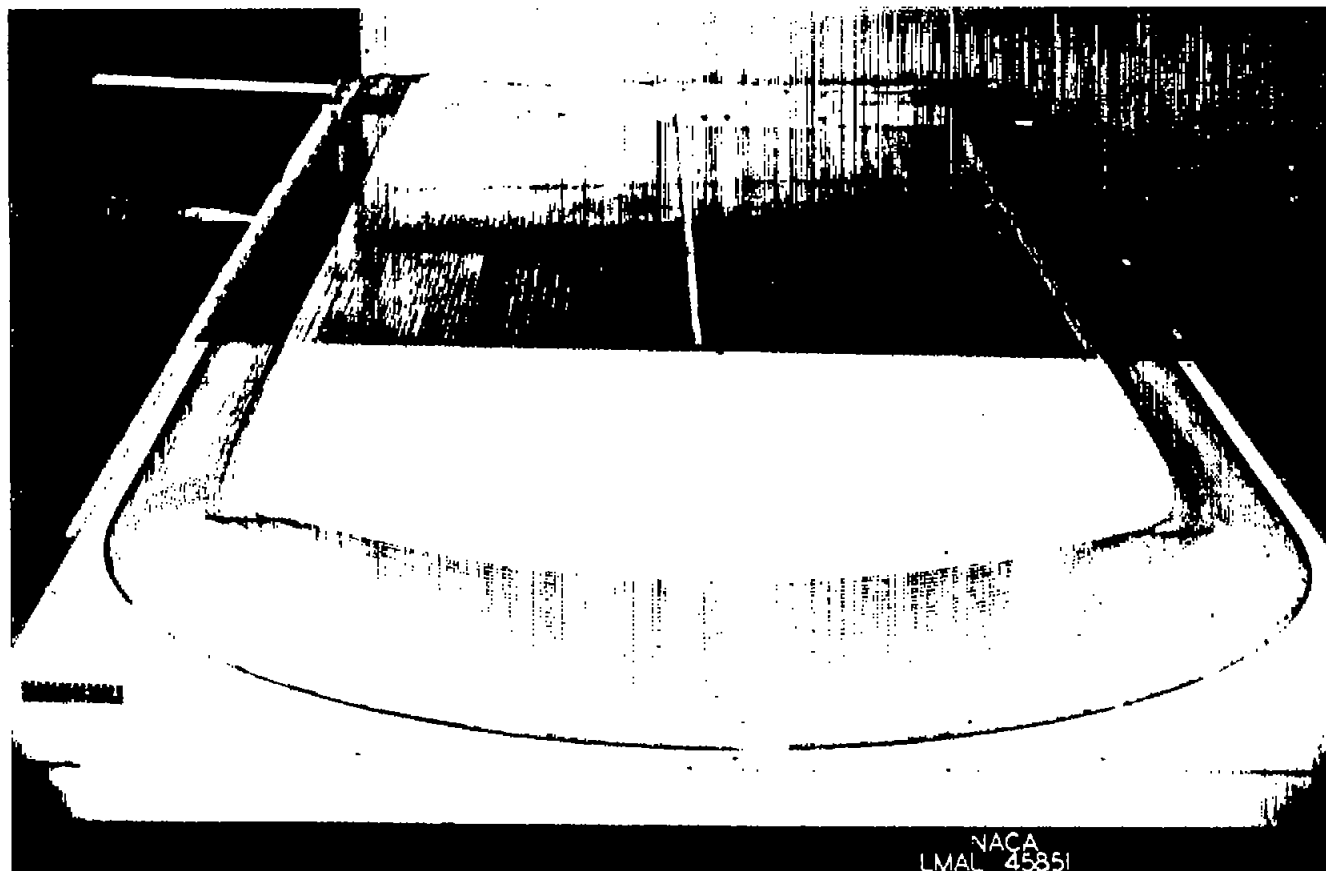
Figure 6.- Electromagnetic-analogy model simulating a thin elliptic tail surface of aspect ratio 3 with a 0.5-chord 0.85-span plain elevator.

Fig. 6
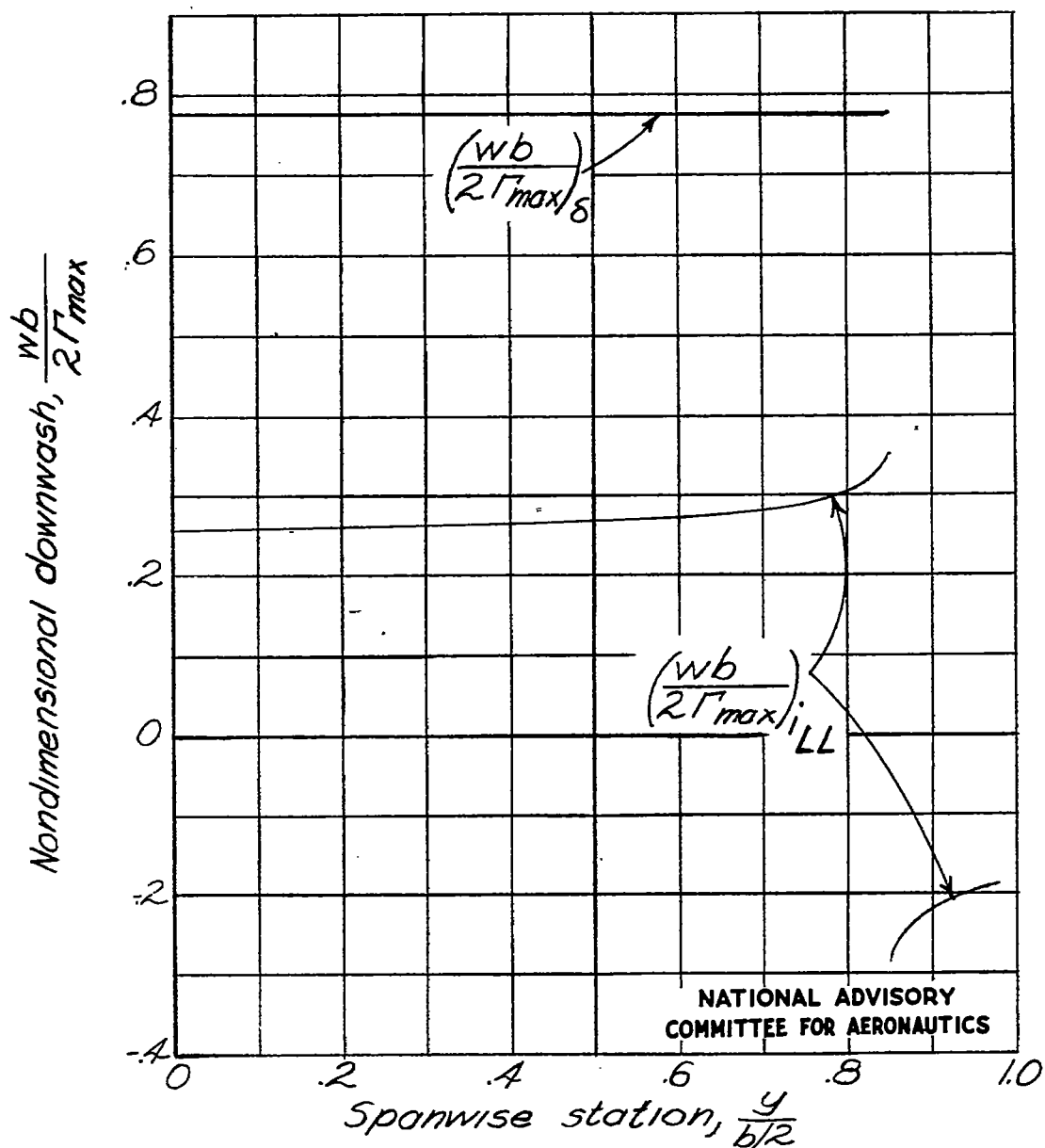
Figure 7 - Values of the nondimensional downwash
parameters $(wb/2\Gamma_{max})_\delta$ and $(wb/2\Gamma_{max})_{i_{LL}}$
calculated for a thin elliptic wing of aspect ratio
3 with a 0.5-chord elevator. Lifting-line-theory
loading of figure 1.

Fig. 8   NACA TN No. 1275
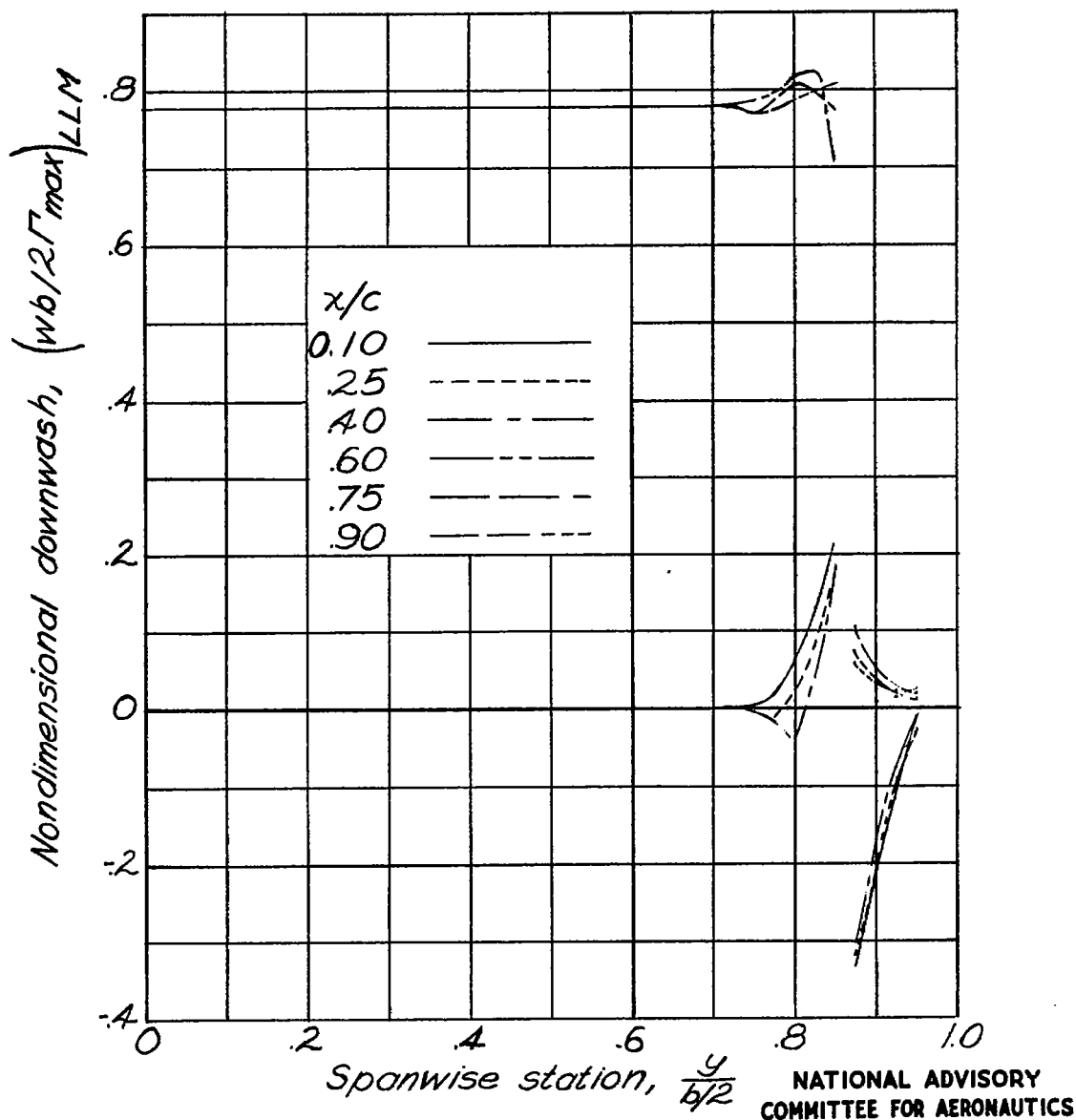
Figure 8.- The nondimensional downwash $(wb/2\Gamma_{max})_{LLM}$ calculated by the two-dimensional theories for a thin elliptic wing of aspect ratio 3 with a 0.5-chord 0.85-span plain flap. Modified lifting-line-theory loading of figure 3.
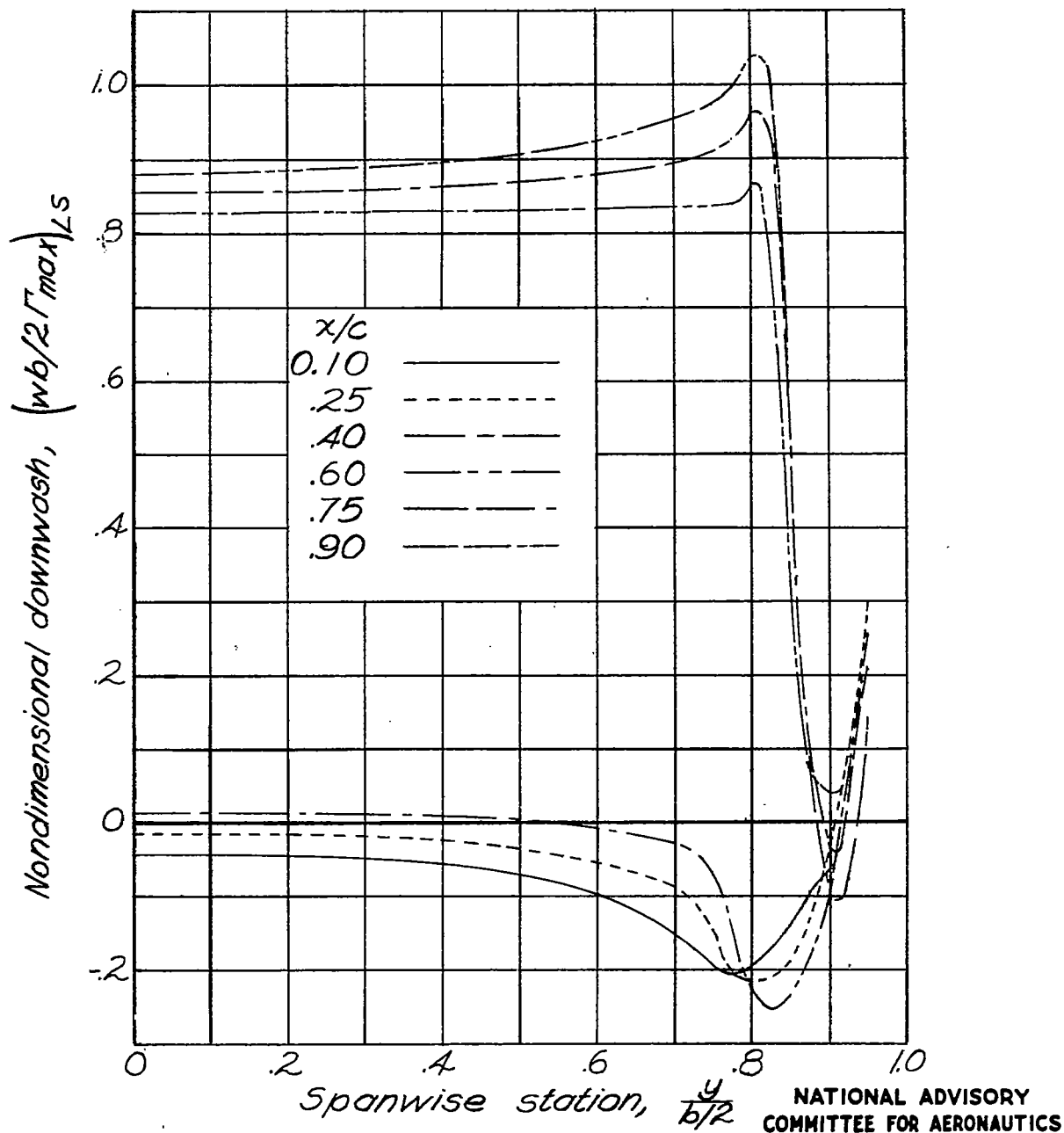
Figure 9.- The nondimensional downwash $(wb/2\Gamma_{max})_{LS}$ determined from the electromagnetic-analogy model of figure 6 for a thin elliptic wing of aspect ratio 3 with a 0.5-chord 0.85-span plain elevator.

Fig. 10   NACA TN No. 1275
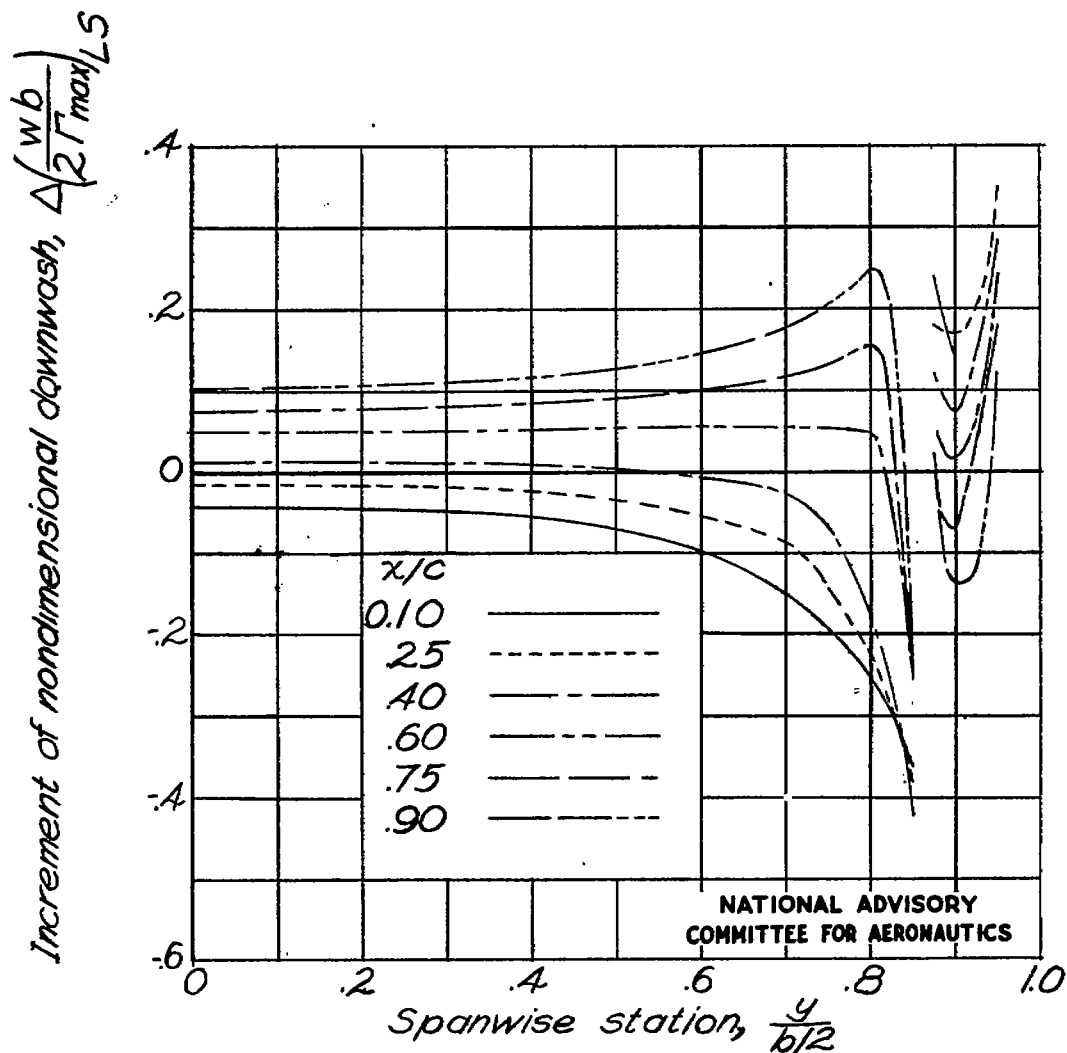
Figure 10.- The increment of nondimensional downwash
$$\Delta\left(\frac{wb}{2\Gamma_{max}}\right)_{LS} = \left(\frac{wb}{2\Gamma_{max}}\right)_{LS} - \left(\frac{wb}{2\Gamma_{max}}\right)_{LLM}$$ for a thin elliptic wing of aspect ratio 3 with a 0.5-chord 0.85-span plain elevator.
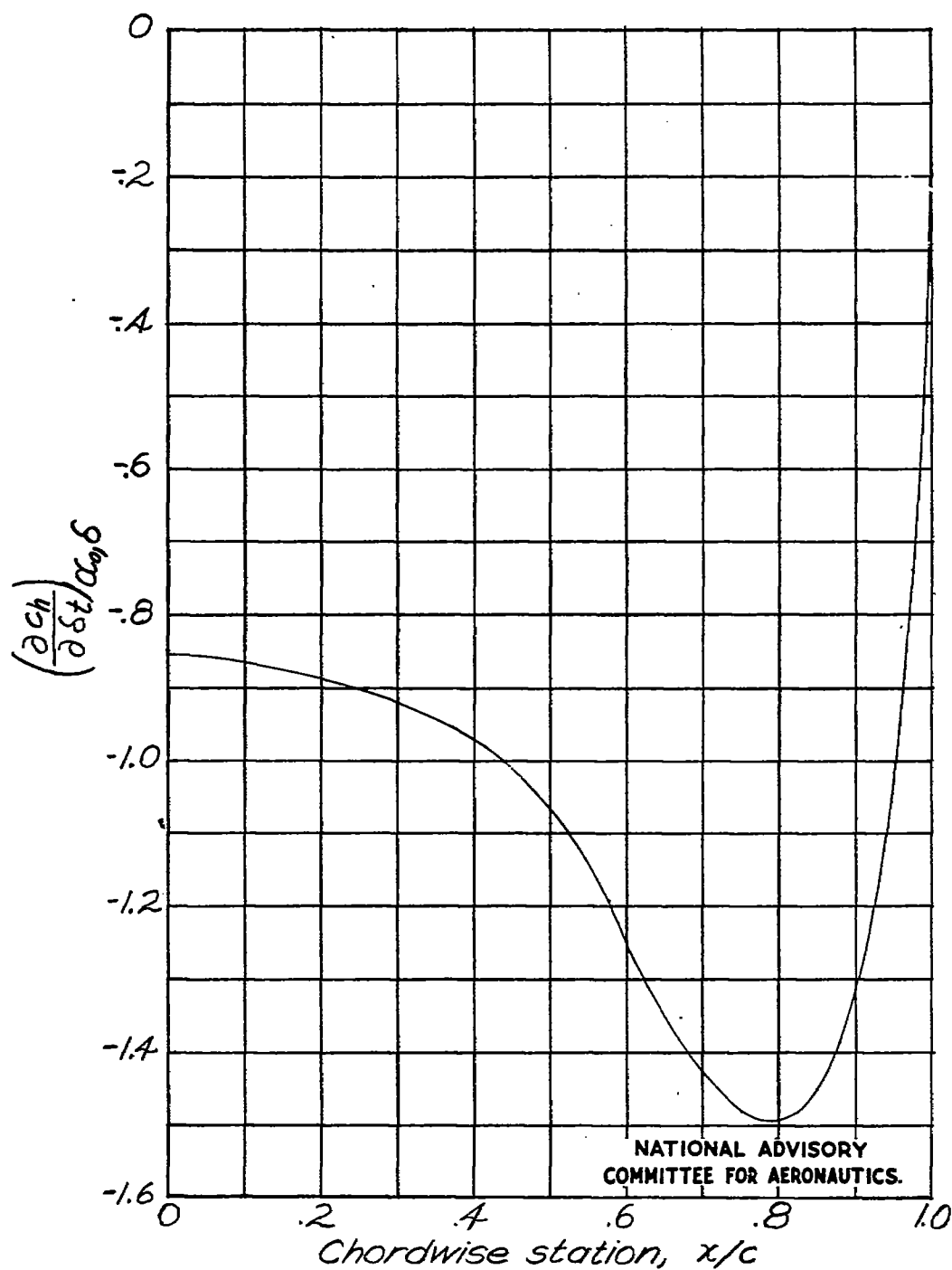
Figure 11.- Variation of parameter $\left(\frac{\partial c_h}{\partial \delta_t}\right)_{\alpha_0,\delta}$ with chordwise location of tab hinge for a 0.5-chord plain flap determined from thin-airfoil theory.

Fig. 12   NACA TN No. 1275
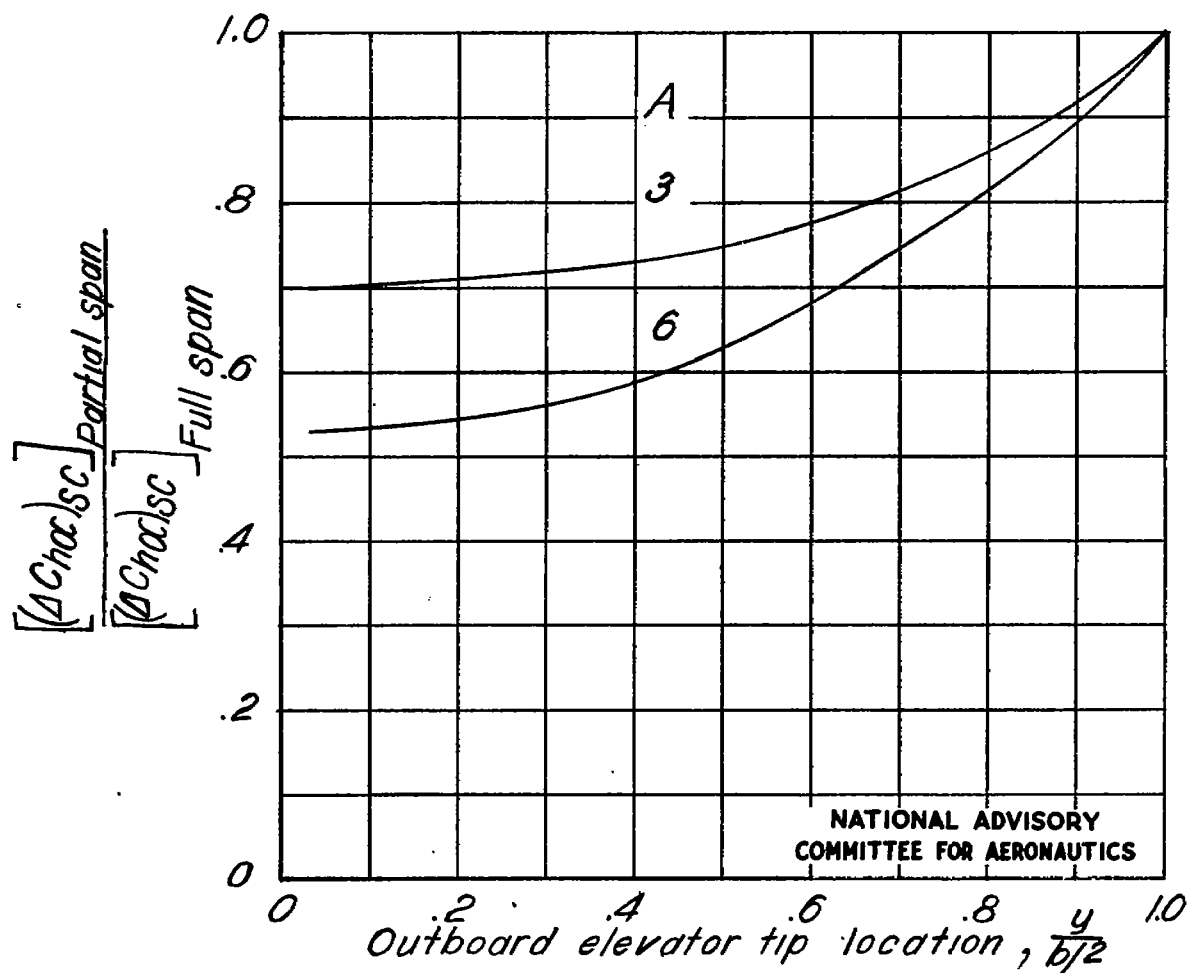
Figure 12.— Effect of partial span on the stream-
line-curvature correction to $C_{h\alpha}$ for elevators.
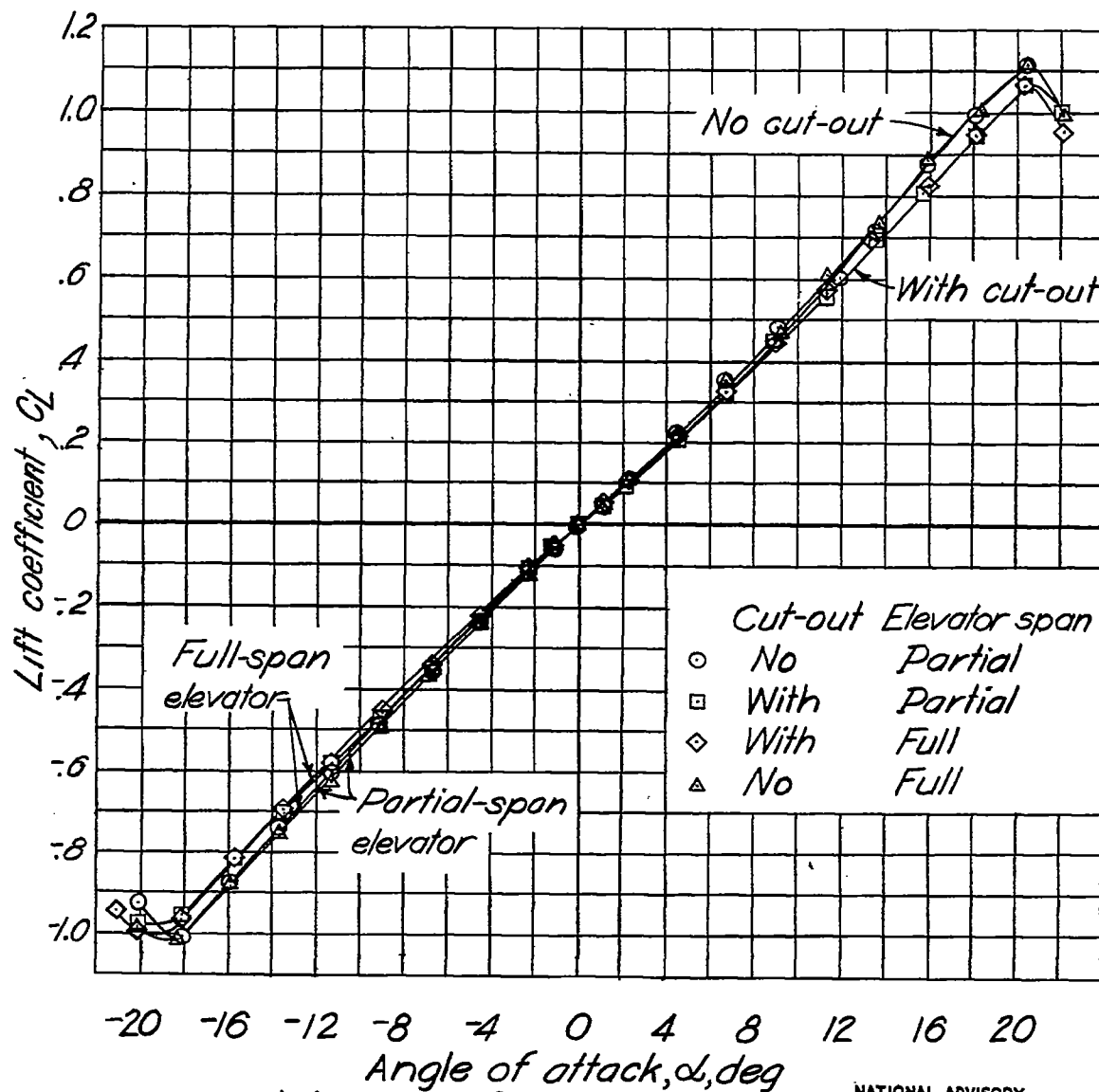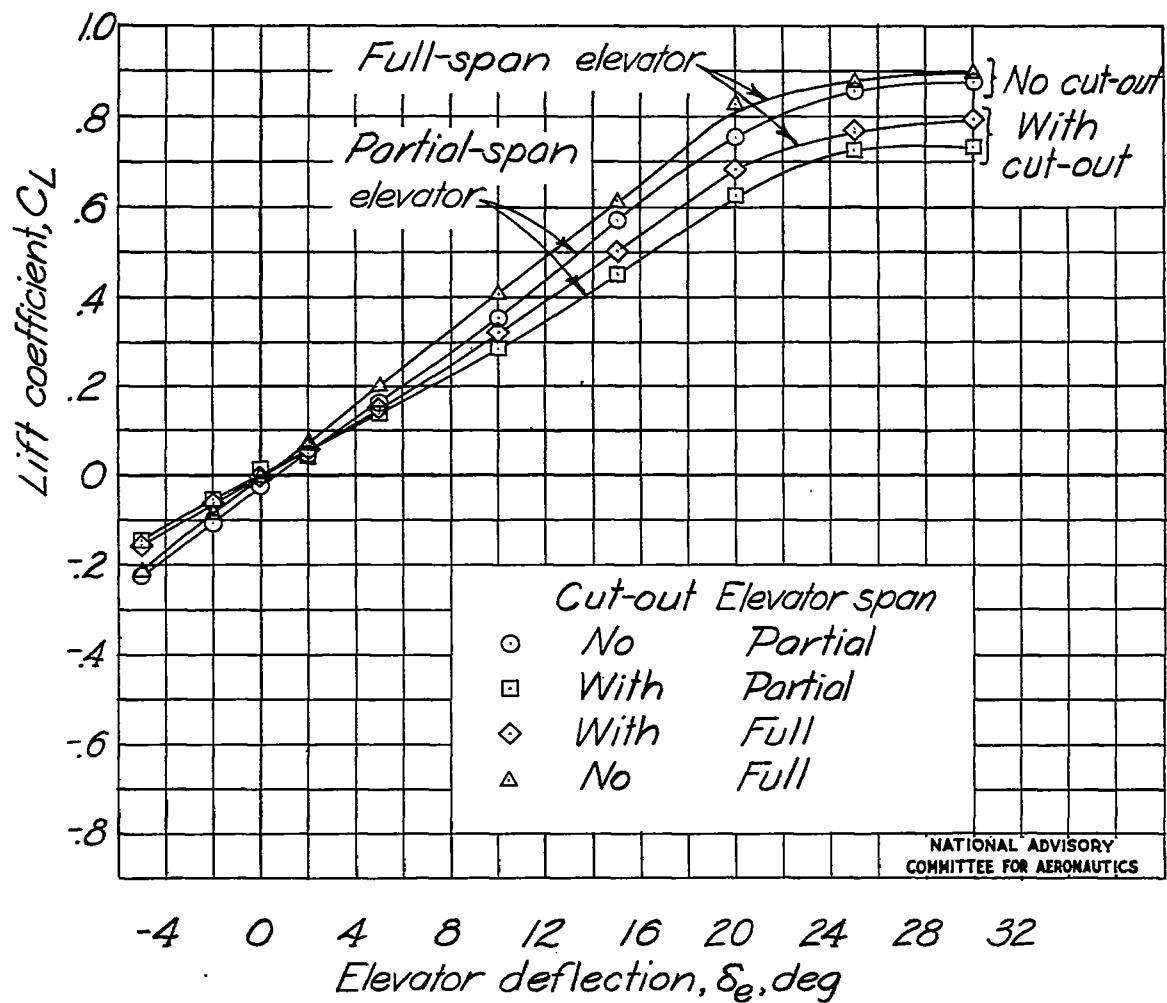
(a) Sealed gap; $\delta_e = 0°$.

Figure 13.—Aerodynamic characteristics of an elliptic semi-span horizontal tail surface with a partial-and full-span 0.50c plain elevator and with and without cut-out. q=13 pounds per square foot; A=3.
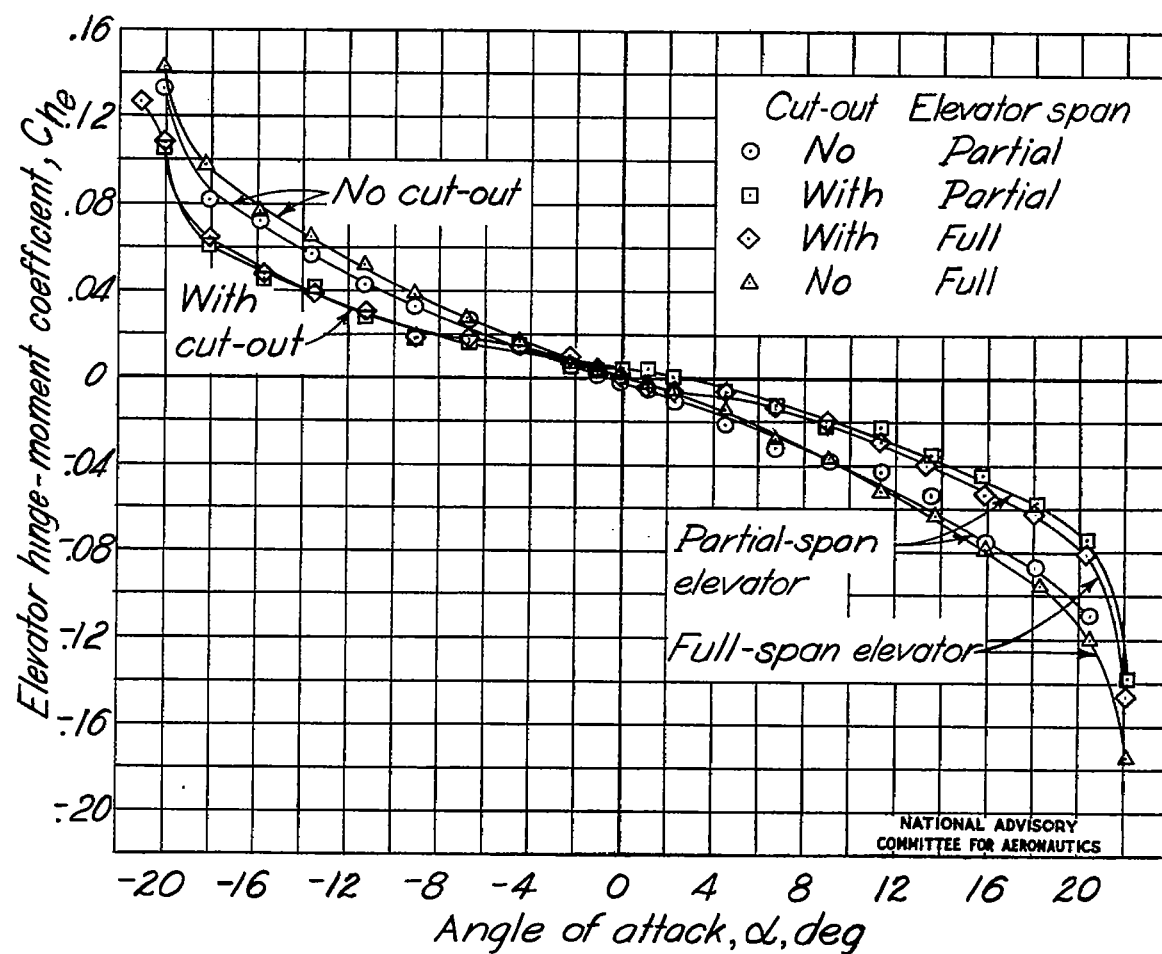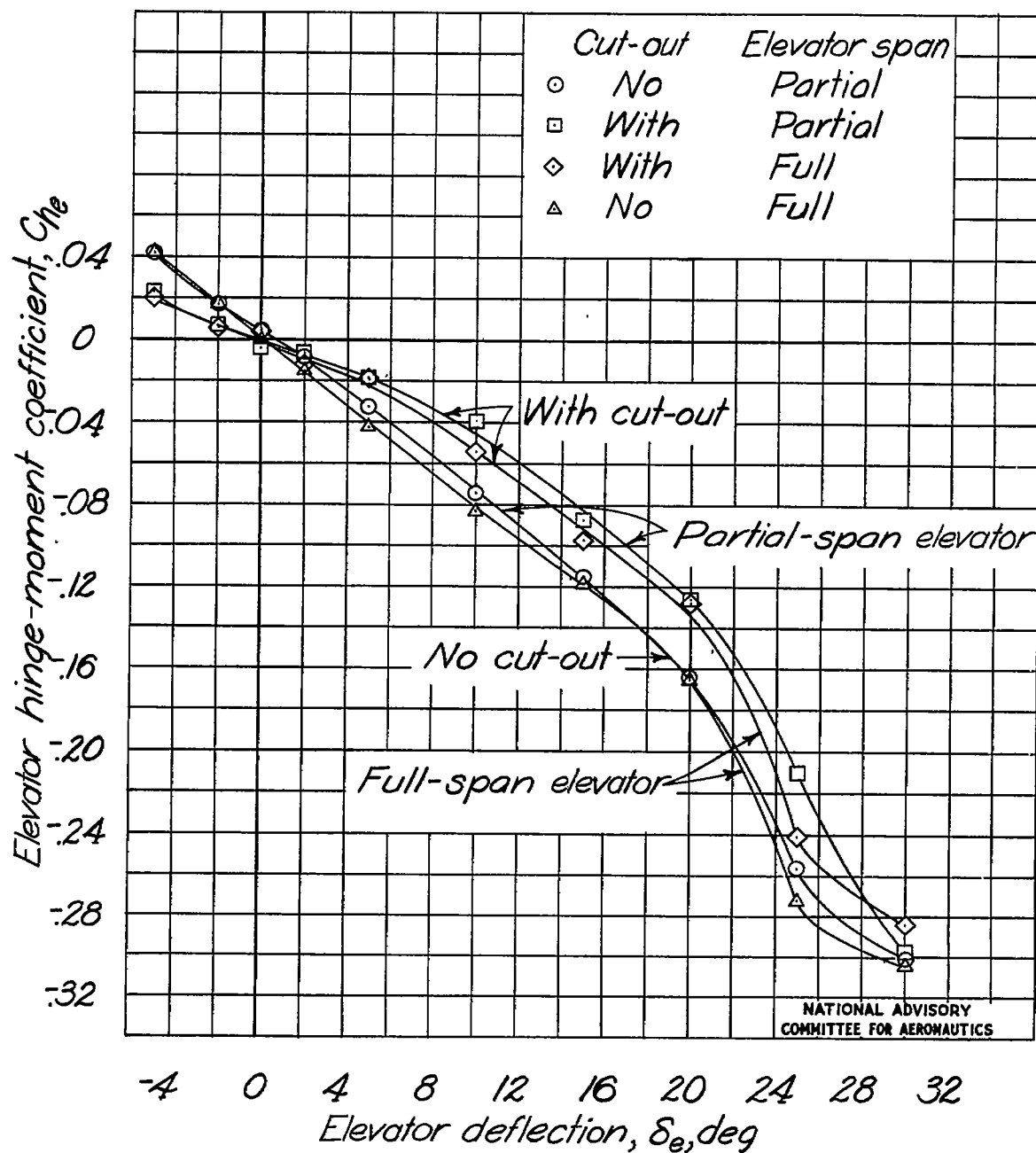
(a) Continued. Sealed gap; $\delta_e = 0°$.

Figure 13.- Continued.

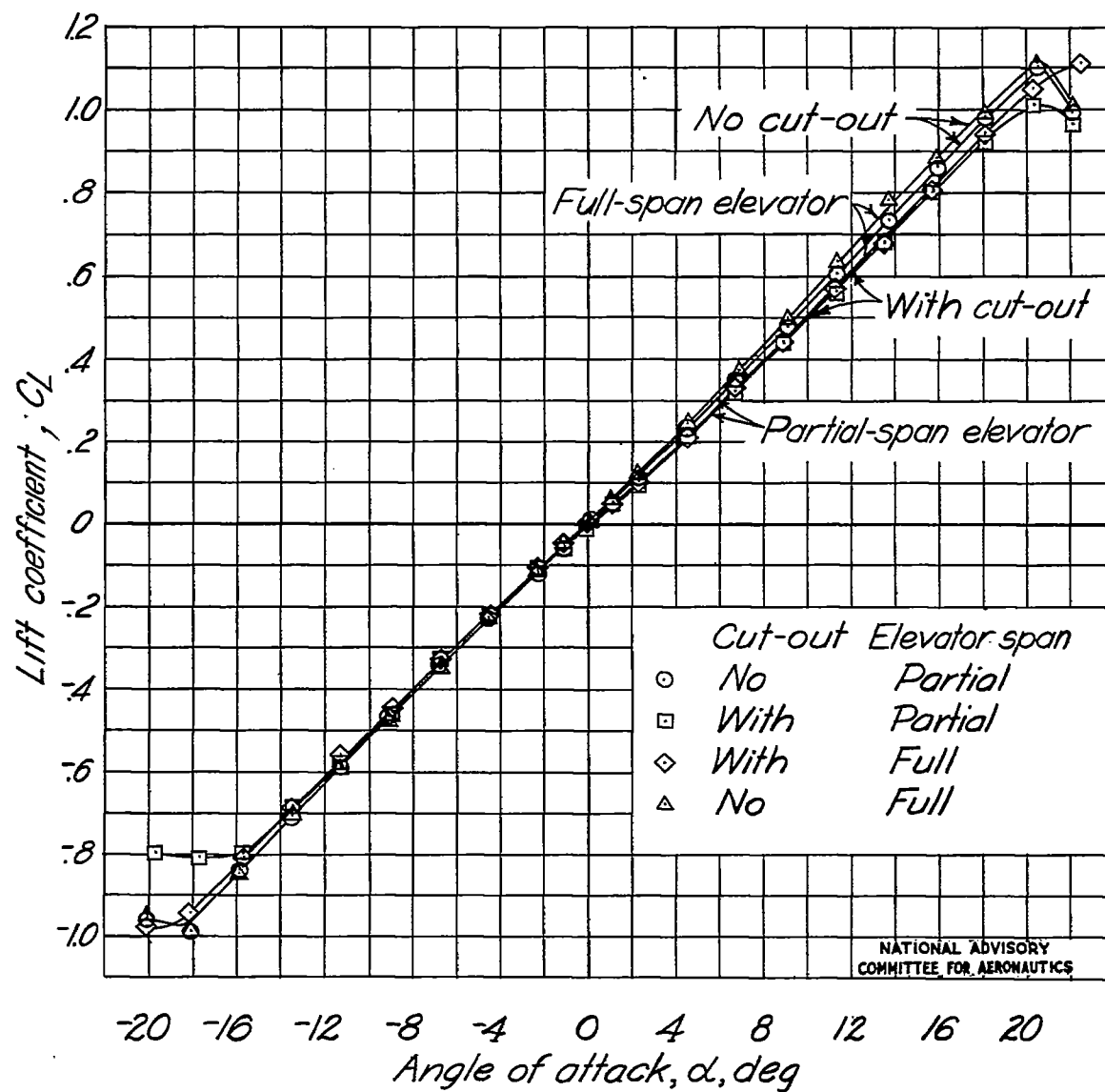(a) Continued. Sealed gap; $\alpha = 0°$.

Figure 13.-Continued.

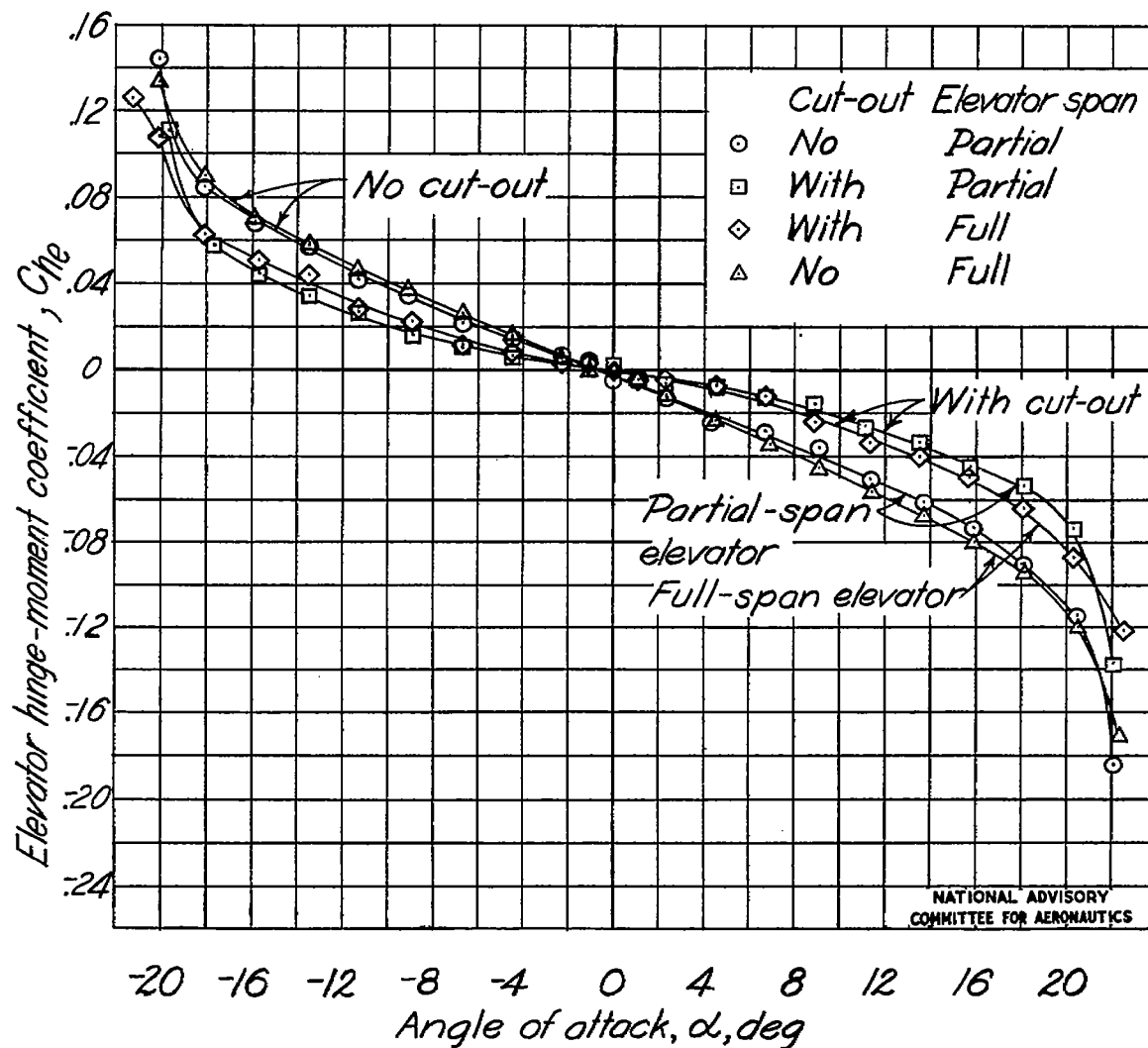|	Cut-out	Elevator span
⊙	No	Partial
⊡	With	Partial
◇	With	Full
△	No	Full

With cut-out

Partial-span elevator

No cut-out →

Full-span elevator

NATIONAL ADVISORY
COMMITTEE FOR AERONAUTICS

Elevator hinge-moment coefficient, C_{h_e}

Elevator deflection, δ_e, deg

(a) Concluded. Sealed gap; $\alpha = 0.^\circ$

Figure 13.- Continued.
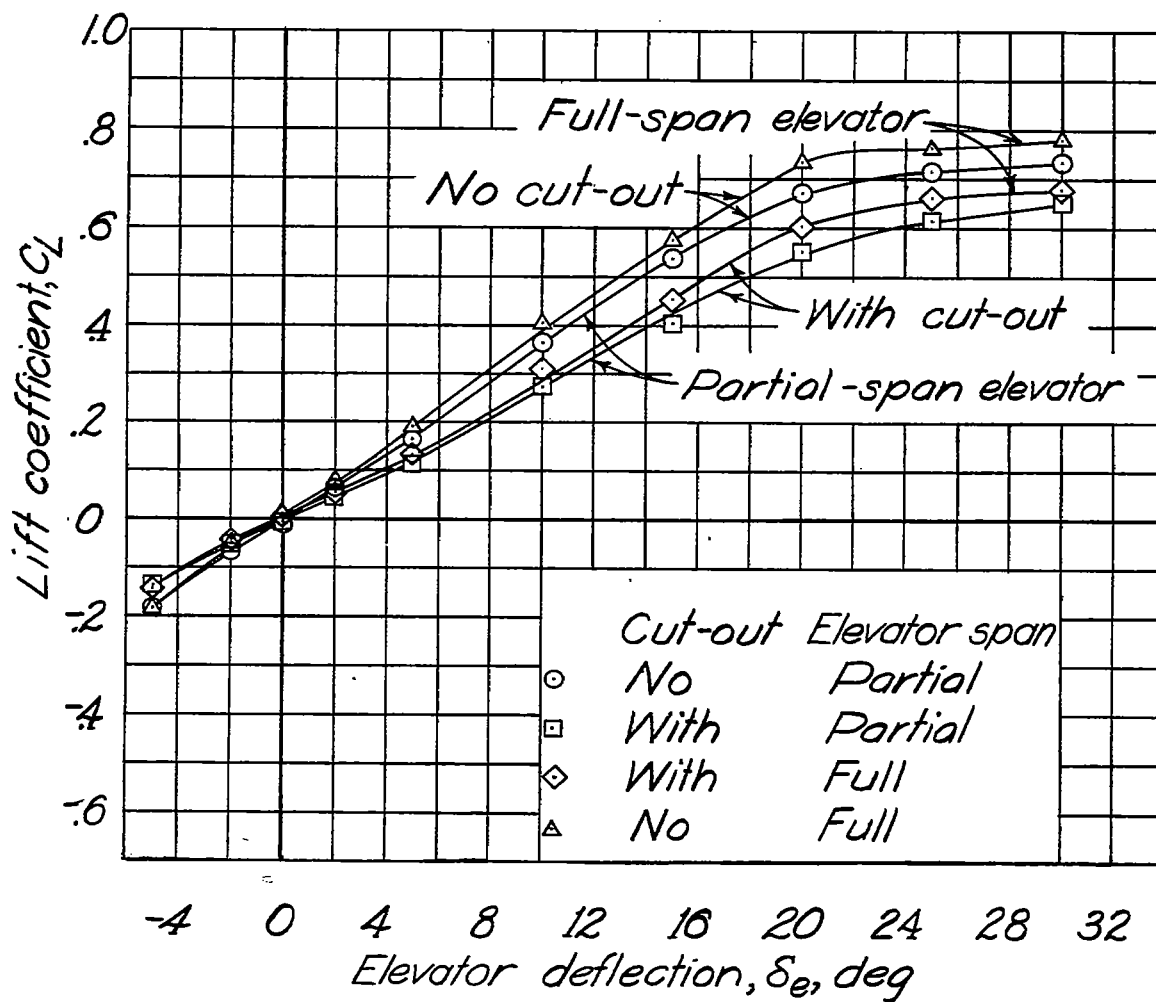
(b) 0.005c gap; $\delta_e = 0°$.
Figure 13.—Continued.

(b) Continued. 0.005c gap; $\delta_e = 0°$.

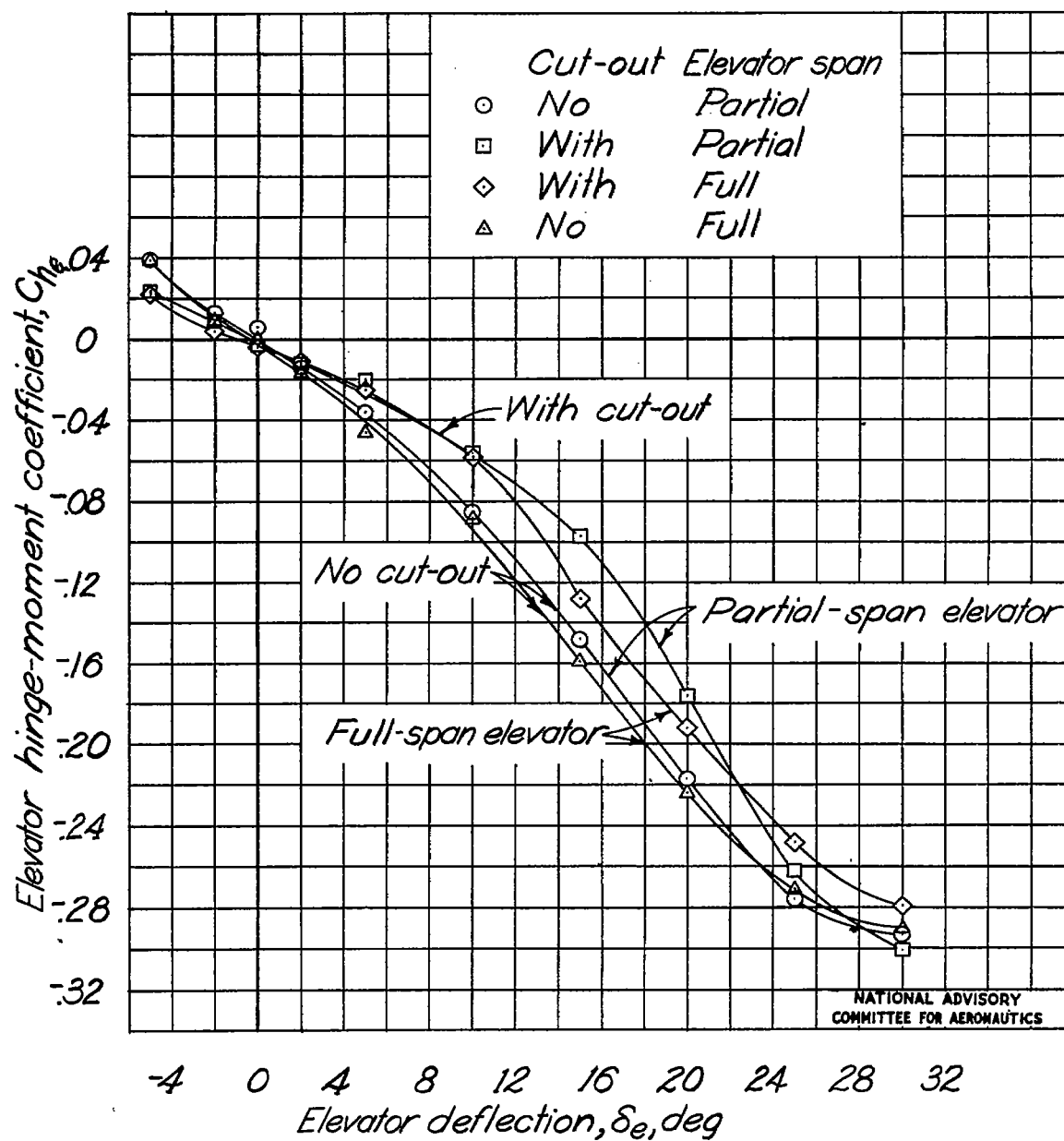Figure 13.-Continued.

(b) Continued. 0.005c gap; $\alpha = 0°$

Figure 13.-Continued.

(b) Concluded. 0.005c gap ; $\alpha = 0°$.

Figure 13.- Concluded.

Full-span elevator

Section A-A

Full-span elevator with cut-out

Leading edge

Reflected image

Tunnel wall

Gap=⁵⁄₃₂"

Elevator nose gap fabric sealed or open · 0.005c

Elevator hinge axis

Gap=¹⁄₃₂"

Partial-span elevator

View B-B

Partial-span elevator with cut-out
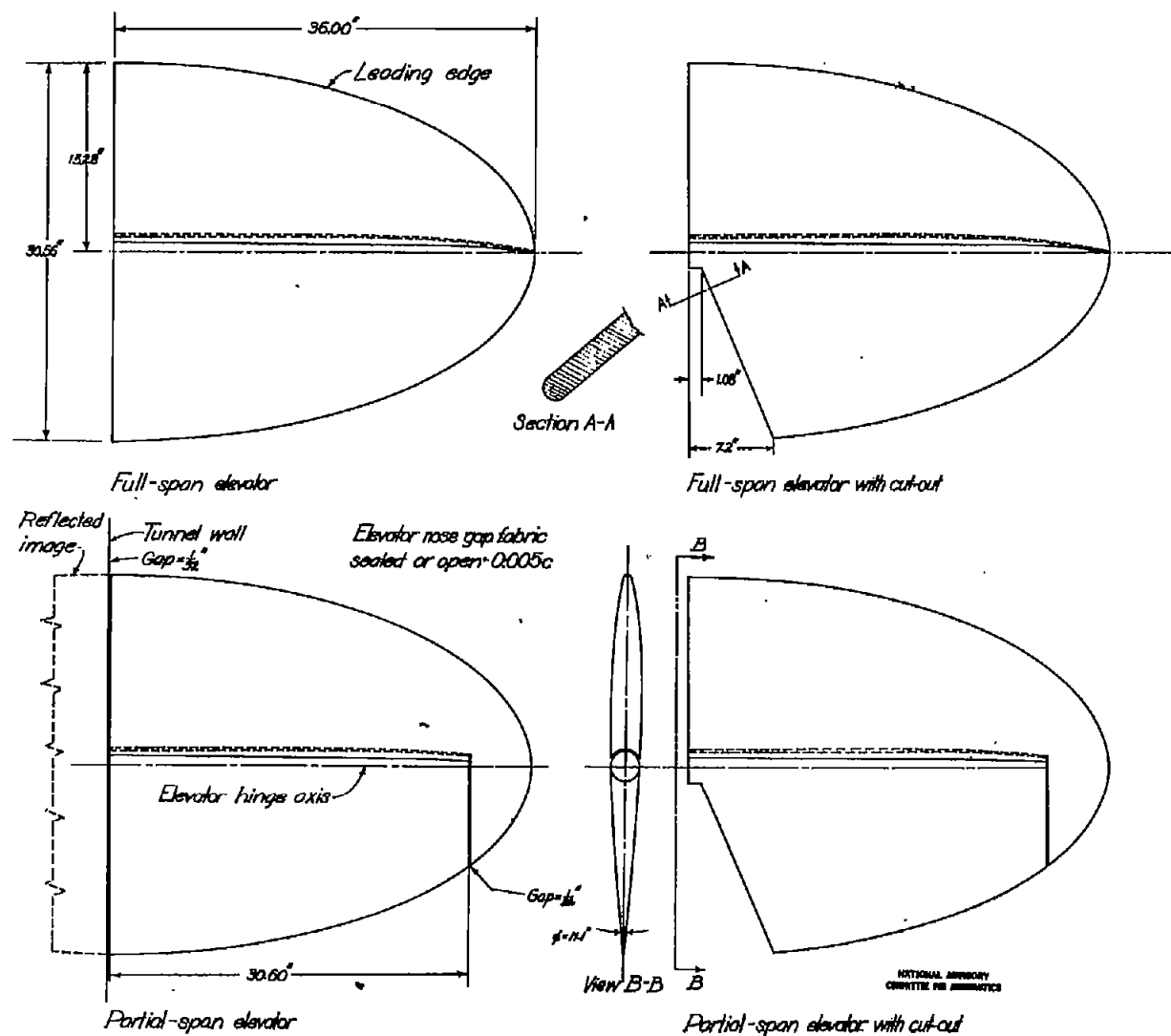
NATIONAL ADVISORY
COMMITTEE FOR AERONAUTICS

Figure 14.- Details of an elliptic semispan horizontal tail surface with a partial-and full-span 0.50c plain elevator with and without cut-out. NACA 0009 section; Aspect ratio =3; area=6 square feet without cut-out, 5.60 square feet with cut-out.

Fig. 14